AUTHOR QUERIES

AUTHOR PLEASE ANSWER ALL QUERIES

PLEASE NOTE: We cannot accept new source files as corrections for your article. If possible, please annotate the PDF proof we have sent you with your corrections and upload it via the Author Gateway. Alternatively, you may send us your corrections in list format. You may also upload revised graphics via the Author Gateway.

Carefully check the page proofs (and coordinate with all authors); additional changes or updates WILL NOT be accepted after the article is published online/print in its final form. Please check author names and affiliations, funding, as well as the overall article for any errors prior to sending in your author proof corrections.

AQ:1 = Please note that the phrases "Energy Efficient Multi-Channel" has been replaced with "Energy-Efficient Multichannel" and "IoT Enabled" has been replaced with "IoT-Enabled" in the title (as per style), which may be a discrepancy from the original submission. Kindly check and confirm.

AQ:2 = Please provide the expansions for the acronyms CSMA/CA and TDMA.

AQ:3 = Please confirm or add details for any funding or financial support for the research of this article.

AQ:4 = Please provide the location for Advanced Sensor Networks (ASN) Research Group and hearX Group (Pty) Ltd.

Energy-Efficient Multichannel Hybrid MAC Protocol for IoT-Enabled WBAN Systems

Damilola D. Olatinwo, Adnan M. Abu-Mahfouz, *Senior Member, IEEE*, Gerhard P. Hancke, *Fellow, IEEE*, and Hermanus C. Myburgh, *Member, IEEE*

***Abstract*—Internet-of-Things (IoT)-enabled wireless body area networks (WBANs) are resource-constrained in nature (energy, bandwidth, and time-slot resources); hence, their performance in healthcare monitoring often deteriorates as the number of active IoT devices sharing the network increases. Consequently, improving the network efficiency of IoT-enabled WBAN systems is essential for improving healthcare monitoring. Hence, we propose an energy-efficient multichannel hybrid medium access control (MAC) (MC-HYMAC) protocol that combines the benefits of the CSMA/CA and TDMA protocols to improve the overall performance of IoT-enabled WBAN systems. We also proposed an adaptive power control scheme, time-slot management scheme, channel utilization mechanism, and dynamic back-off time policy to improve the overall network efficiency. In addition, we applied a finite-state discrete-time Markov model to determine the traffic arrival pattern and analyze the transition states of biomedical devices to facilitate optimal decision-making for enhanced overall performance of the network. Standard metrics, such as energy efficiency, throughput, delay, packet drop ratio, and network lifetime, were used to evaluate and compare the existing MAC protocols.**

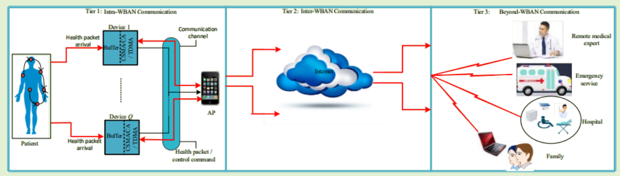

***Index Terms*—Adaptive power control, channel selection, CSMA/CA, discrete-time Markov model, IEEE 802.15.4, Internet of Things (IoT), medium access control (MAC) protocol, multichannel, TDMA, wireless body area network (WBAN).**

I. INTRODUCTION

THE advent of the Internet-of-Things (IoT) technology has been enhancing the popularity of various wireless systems, such as wireless body area networks (WBANs), as a result of its positive impacts [1]. IoT can be applied to different domains, such as healthcare monitoring [1], structural health monitoring [2], environmental monitoring (e.g., water quality monitoring and weather monitoring) [3], and industry (e.g., manufacturing and transportation systems) [4], to create smart systems. For instance, integrating IoT into structural health monitoring helps to continuously collect data from different sensors deployed on structures (e.g., buildings, railway tracks, and bridges). With such data, important information regarding the current state of different structures can be extracted for safety and maintenance purposes. Integrating IoT into water monitoring can help to create a smart water quality monitoring system that can assist in monitoring changes in water quality to prevent the distribution of unclean water to consumers. In addition, the integration of IoT in industries, such as transportation, helps to create intelligent transportation systems that can enable transportation authorities to track vehicle locations, predict future locations, and predict current road traffic. Similarly, combining an IoT technology with WBAN helps to provide cost-effective services and minimizes frequent hospital visits. Therefore, integrating IoT technologies into WBANs is advantageous for healthcare monitoring to improve patients' overall health and well-being.

An IoT-enabled WBAN is a special type of network designed for healthcare applications and operates independently to manage the communications between various biomedical devices that are positioned in, on, and around the patient's body. IoT WBAN enables the near real-time monitoring of patients' health status and health diagnosis, and also helps with patients' information management for

Manuscript received 9 September 2023; revised 21 September 2023; accepted 21 September 2023. This work was supported by the Council for Scientific and Industrial Research, Pretoria, South Africa, through the Smart Networks Collaboration Initiative and the IoT-Factory Program (funded by the Department of Science and Innovation (DSI), South Africa). The associate editor coordinating the review of this article and approving it for publication was Prof. Bin Gao. *(Corresponding author: Damilola D. Olatinwo.)*

Damilola D. Olatinwo and Hermanus C. Myburgh are with the Department of Electrical, Electronic and Computer Engineering, University of Pretoria, Pretoria 0002, South Africa (e-mail: damibaola@gmail.com; herman.myburgh@up.ac.za).

Adnan M. Abu-Mahfouz is with the Department of Electrical, Electronic and Computer Engineering, University of Pretoria, Pretoria 0002, South Africa, and also with the Council for Scientific and Industrial Research (CSIR), Pretoria 0184, South Africa (e-mail: a.abumahfouz@ieee.org).

Gerhard P. Hancke is with the Department of Computer Science, City University of Hong Kong, Hong Kong, SAR (e-mail: gp.hancke@cityu.edu.hk).

Digital Object Identifier 10.1109/JSEN.2023.3322627

decision-making purposes. The IoT-enabled WBAN biomedical devices are responsible for sensing and communicating sensed physiological signals obtained from the patient's body to remote medical centers by leveraging IoT technologies. However, because these devices are small, they have limited resources, including limited battery power [5]. Therefore, to manage the limited resources and prolong the lifetime of biomedical devices, it is essential to address energy wastage, time wastage, and channel utilization issues. It is noteworthy that, among the modules of the biomedical devices, the communication module consumes more energy during data transmission. Hence, it is essential to manage energy resources during data transmissions through the design of an efficient medium access control (MAC) protocol. In IoT-enabled WBANs, the biomedical devices share a communication channel for health packet transmission. This shared communication channel is typically regulated by the MAC protocol [5], [6]. This further indicates that MAC design is key to achieving an energy-efficient IoT-enabled WBAN system. Such a system can be achieved by leveraging the optimization of the MAC protocols to meet the system's quality-of-service (QoS) requirements (such as energy efficiency, low delay, high reliability, and high throughput) using limited resources while simultaneously maintaining high network utilization. Through research efforts, a few solutions have been proposed to address energy and time-slot wastage issues in WBAN using MAC protocols [7], [8], [9], [10], [11].

Unfortunately, existing solutions are yet to fully address these issues. Generally, most conventional WBAN MAC protocols are designed and developed to operate only on a single channel, i.e., the biomedical devices have only one single channel available for all communications [12], [13], [14], [15]. In such a system, determining which of the devices to access the channel first becomes very difficult, and this could greatly limit the data transportation capacity of the network, consequently resulting in the low acceptance and productivity of the IoT-enabled WBAN system for healthcare monitoring applications. Therefore, to address these research concerns, this study proposes the design of an energy-efficient multichannel hybrid MAC (MC-HYMAC) protocol combined with different novel resource management strategies for IoT-enabled WBAN systems.

The proposed WBAN system was built on a multichannel mechanism that employs multiple channels, i.e., one channel is used as the control channel, the rest of the channels are used as the data channels, and the data channels are used by biomedical devices for transmitting health packets. Based on the QoS requirements of IoT-enabled WBAN systems, biomedical devices in the network are categorized into two categories based on their health packets: category 1 and category 2. Category 1 devices are assumed to have critical health packets, whereas Category 2 devices are assumed to have less-critical health packets. Critical health packets are emergency-based data packets and are required to be delivered in a timely manner, whereas less-critical health packets are normal and periodic data packets. To improve the performance and solve channel starvation issues, we devised the use of different channels. This enables the devices in the network to use separate channels for their communications. Using a separate channel helps to minimize collisions among the devices, minimize delay, and improve energy efficiency and system throughput. Furthermore, to achieve an energy-efficient and reliable WBAN network, an adaptive power control scheme, a time-slot management strategy, and a dynamic back-off time policy were proposed. Also, a discrete-time Markov model that has a finite buffering capacity for storing the arrival requests of the devices was introduced. Therefore, to improve the existing hybrid CSMA/CA and TDMA protocols based on their shortcomings, such as channel utilization, energy consumption, time slot, energy wastage, and delay issues, the following contributions were made in this study.

1) An energy-efficient MC-HYMAC protocol for IoT-enabled WBAN systems. To improve energy efficiency and prolong the overall network lifetime, separate channels for the devices' health packet transmission and AP control signal transmission were employed.
2) The integration of edge AI with IoT-enabled WBAN system for near real-time communication.
3) An efficient channel mapping mechanism for the WBAN biomedical devices. This mechanism helps the devices know when to transmit their health packets to minimize issues such as collision, delay, and energy consumption in the network.
4) An adaptive power control scheme to reduce energy wastage in IoT-enabled WBAN systems.
5) A dynamic time-slot allocation scheme and a back-off time scheme for the efficient utilization of the IoT-enabled WBAN channels.
6) A novel strategy to minimize delay and packet drop ratio, and increase the network lifetime and energy efficiency without affecting the throughput of the IoT-enabled WBAN system.
7) A finite-state discrete-time Markov model to determine the traffic arrival pattern and analyze the transition states of the biomedical devices and the state of the channel for decision-making purposes in order to improve the lifetime of the network.

The remainder of this study is structured as follows. Section I introduces this study. Section II presents a literature review of existing MAC protocols. The system architecture, mathematical model, channel mapping mechanism, channel selection policy, back-off time policy, and the time-slot management scheme are presented in Section III. Section IV presents the Markov model analysis. Section V presents a performance analysis of the proposed system in terms of energy consumption, throughput, and delay. The operation and description of the proposed protocol are presented in Section VI. Section VII presents the simulation results. Section VIII concludes this article.

II. Related Studies

First, in this section, various research articles on energy-efficient WBAN systems based on single-channel MAC protocols are presented, followed by an exploration of WBAN systems developed on multichannel MAC protocols. An example of an MAC protocol designed based on a single channel is [11]. The authors of this study proposed an energy-aware MAC protocol for IoT-enabled WBAN systems. They employed a transmission scheduling mechanism to duty-cycle the operations of devices to improve the energy efficiency of the network. However, because this protocol is based on a single channel, more delay and energy consumption are experienced during data transmission, owing to collisions that cause several retransmissions (ReTs). Although the system employed a sleep-wake-up mechanism to increase the lifetime of the network, the problem of channel starvation experienced by devices with less-critical health packets during data transmission was not addressed. In addition, the data packets generated by these devices are usually in large amounts, and because they have limited channel access, most health packets are either dropped off or lost. Consequently, the system became unreliable. In contrast to [11], we proposed a multichannel WBAN protocol that uses separate channels for device health packet transmission and AP control signal transmission. To enhance the efficiency of the network, we proposed a channel mapping mechanism and channel selection policy for the devices in the network to efficiently make use of the channels.

Zhang et al. [15] proposed an asynchronous duty cycle mechanism to minimize collisions and energy consumption of the WBAN system. However, this work focused on a homogeneous-based WBAN system. Another homogeneous-based WBAN system was proposed in [16] based on the system and different energy-saving strategies, which includes moving the major overhead transmissions to the personal server, introducing a waiting order state, and enabling a retransmission process at the end of all transmissions to reduce the waiting order time and save energy. However, more packet transmission delays were experienced, which reduced the overall system throughput. In contrast to [15] and [16], we propose an MC-HYMAC protocol that can cater to the heterogeneity of WBAN systems. In addition, a channel mapping mechanism, channel selection policy, and dynamic time slot allocation scheme were proposed to enhance the overall performance of the system.

Sun et al. [17] proposed a priority-based MAC protocol to improve the efficiency of the WBAN systems. The devices in the network are prioritized based on their degree of importance, timeout conditions, remaining energy, and sampling rate. The total number of device time slots and conflicting time slots was adjusted to improve the average packet delivery rate. In addition, a time-slot allocation algorithm was proposed based on a greedy strategy to improve network performance. The algorithm assigns a guaranteed time slot to devices with high priorities.

Thirumoorthy et al. [18] proposed an energy-efficient distributed queuing MAC protocol for WBANs. The system employed a distributed queuing technique to enhance radio channel utilization. In contrast to [17] and [18], we propose a multichannel MAC protocol to improve the energy efficiency of IoT-enabled WBAN systems. In addition, different resource management strategies have been proposed to efficiently utilize limited WBAN resources, such as energy, time slot, and bandwidth. For instance, we proposed an adaptive power control scheme to prevent energy wastage, a channel mapping mechanism, a channel selection policy for efficient channel utilization, and a dynamic time-slot allocation scheme to prevent time-slot wastage.

Employing a single-channel MAC protocol may not be efficient in addressing issues such as energy wastage, delays, and collisions in WBANs. Thus, we reviewed relevant research that employed multichannel MAC protocols to improve WBAN systems. In this direction, Cho et al. [19] proposed a single radio multichannel MAC protocol to improve the energy efficiency and reliability of the system, and minimize delay using a data aggregation technique. However, the data aggregation technology is only suitable for homogeneous WBAN systems.

Another multichannel MAC protocol was proposed in [20] to mitigate interference and minimize delays in WBANs. A channel mapping technique was employed to determine the channel availability to improve the performance of the system. However, the back-off time policy, power control, and time-slot allocation mechanisms were not considered. Moreover, the transition states of the devices were not analyzed.

Kirbas et al. [21] designed a multichannel MAC protocol to improve the energy efficiency of WBANs. To achieve this, a collision prevention technique was employed to reduce the device contention period, thereby minimizing the delay. In this study, several devices acted as hubs to aggregate demand. However, updating the real-time information of devices increases their energy consumption, which, in turn, affects network lifetime. In addition, channel mapping and selection mechanisms were not considered, resulting in a high delay in determining which device would access the channel first. In addition, the MAC protocol was designed only for homogeneous WBAN.

A multichannel TDMA-based MAC protocol was proposed in [22] to address the energy consumption issue. A channel-mapping technique was employed to analyze the states of the channel to prevent collisions. In addition, a collision avoidance mechanism was proposed to mitigate interference and enhance the efficiency of the system. Nevertheless, the power control and allocation scheme, back-off time policy, and time-slot management scheme were not considered; thus, the likelihood of energy wastage and shortened lifespan of the devices would occur in this network.

A time-sharing multichannel MAC protocol based on the TDMA scheme for WBAN systems was proposed [23]. In this study, the authors considered a channel selection strategy to mitigate inference, reduce delay, and improve the energy efficiency of the system. Each device in the network was allocated a time slot and channel for data transmission. However, because the protocol was not designed for a single WBAN, the likelihood of collisions was high because a collision-avoidance mechanism was not considered. In addition, methods to efficiently utilize the limited power resources of the WBAN system to avoid energy wastage were not considered.

Rasheed et al. [24] proposed a modified superframe structure (MSS-IEEE 802.15.4) based on the IEEE 802.15.4 standard to address energy consumption and delay problems.

A priority-based CSMA/CA mechanism was employed, and different priorities were allocated to the nodes by adjusting their data size and data type.

Unlike previous studies (e.g., [19], [20], [21], [22], [23], and [24]), we propose a heterogeneous-based MC-HYMAC protocol that combines the benefits of the IEEE 802.15.4 standard, CSMA/CA, and TDMA schemes to prevent collisions and allocate time slots according to the priority of the devices. To effectively and efficiently utilize WBAN-limited resources, we propose novel resource management strategies, such as an adaptive power control and allocation mechanism, a channel selection scheme, and a dynamic back-off time policy. In addition, we employ a finite-state discrete-time Markov model to analyze the device transition states and channel states for accurate decision-making. Based on this model, the probability of moving from one state to another is determined by summing all transition probabilities and their frequencies.

III. Proposed Method

In this section, we present the proposed MC-HYMAC system architecture, mathematical model, channel mapping mechanism, channel modeling, back-off time policy, and the time-slot management scheme in the following.

A. System Architecture

Herein, we propose an MC-HYMAC system consisting of $\mathcal{A}$ WBANs and $\mathcal{B}$ biomedical devices that transmit their health packets in $\mathcal{N}$ different channels. For each WBAN, we assume a heterogeneous scenario, in which the network consists of different types of devices with different roles and capabilities. Some devices act as ordinary biomedical sensor nodes that can only collect and send health data to an access point (AP) that can perform edge AI tasks. Consequently, all the computational overhead and energy consumption that the edge AI would have introduced to individual biomedical devices based on complex tasks related to data collection, processing, analysis, and decision-making were moved to the AP side. In general, the AP acts as a coordinator and local processor. It collects all the sensed health information from biomedical devices through IoT communication technology and stores it temporarily in its buffer. However, to minimize the delays associated with the time spent by the AP in providing services to the devices and considering the time-sensitive nature of the devices, we proposed an edge AI system with mobile edge computing (MEC) device. MEC is a computing paradigm that enables computations at the network edge. It has various advantages, such as low energy consumption, low delay, and high quality of service.

Consequently, we shifted the major computations of the AP to the MEC to reduce the computational time and power of the overall network. MEC has large computational resources, handles computations faster, and is more efficient than the AP. The MEC is deployed at the base station to provide real-time computing services to the WBAN devices. The AP serves as an intermediary between the MEC and devices. Therefore, the MEC forwards the processed health information of the devices to the cloud server and from the cloud server to the hospital server for timely and accurate decision-making [25]. Fig. 1 presents the system architecture of the proposed MC-HYMAC system.

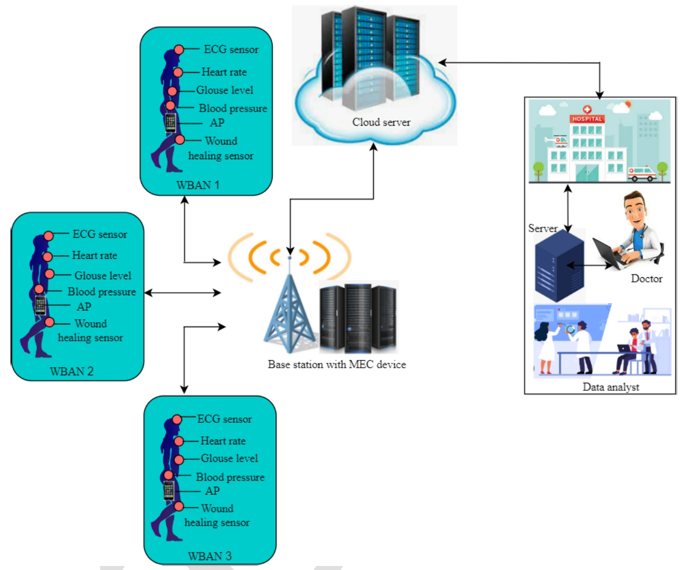

Fig. 1. Proposed MC-HYMAC architecture with MEC.

B. System Model

In each WBAN, one channel is dedicated to the AP for sending control signals, such as the distribution of channels and time slots. Biomedical devices use the remaining channels for health packet transmissions. Biomedical devices are assumed to have two types of health packets: critical and less critical. The critical and less-critical health packets are dynamically grouped into category 1 (C_1) and category 2 (C_2), respectively, based on their data type, payload size, and priority. The critical health packets are emergency-based data that need urgent attention, while the less-critical health packets are normal health data. We assumed that not all the devices in the network have data to send. Therefore, (C_2) devices that have data to send would contend for transmission opportunities using the CSMA/CA protocol. For critical health packet generation, the devices will send an emergency beacon message to the MEC through the AP without contention since they are delay-intolerant. In addition, if the control channel is free and has no available data channels, then the control channels can be used by biomedical devices with critical health packets to transmit their data. The modeling of the proposed MC-HYMAC protocol is based on the following assumptions. In each WBAN, one channel is dedicated to the AP to send control signals, such as the distribution of channels and time slots, while the biomedical devices use the remaining channels for health packet transmissions. Biomedical devices are assumed to have two types of health packets: critical and less critical. The critical and less-critical health packets were dynamically grouped into category 1 (C_1) and category 2 (C_2), respectively, based on their data type, payload size, and priority. Critical health packets are emergency-based data requiring urgent attention, while the less-critical health packets are normal health data. We assumed that not all the devices in the network have data to send. Therefore, (C_2) devices that have data to send would contend for transmission opportunities using the CSMA/CA protocol. For critical health packet generation, the devices send an emergency beacon message to the MEC through the AP without contention because they are delay-intolerant. In addition, if the control channel is free and has no available data channels, then the control channels can be used by biomedical devices with critical health packets to transmit their data. The modeling of the proposed MC-HYMAC protocol is based on the following assumptions.

1) A sense-and-send approach was used.
2) The traffic arrival follows a Poisson process.
3) The devices in the network are assumed to have a fixed power level for a particular state, but, then, different power levels are used across the different states.
4) The devices are assumed to perform two types of operations including the transmission of health packets to the MEC through the AP and the reception of control commands from the MEC through the AP.

C. Mathematical Model

In the proposed MC-HYMAC protocol, the total number of WBANs is modeled as a set of $\mathcal{A} = \{a_1, a_2, \ldots, a_A\}$, the total number of biomedical devices is modeled as a set of $\mathcal{B} = \{b_1, b_2, \ldots, b_B\}$, and the total number of channels is modeled as $\mathrm{CH} = \{\mathrm{ch}_1, \mathrm{ch}_2, \ldots, \mathrm{ch}_{\mathrm{CH}}\}$. Consequently, all the APs in all the WBANs transmit the control signal from the MEC to the biomedical devices using the first channel, denoted by a set of CH, and the remaining CH-1 channels are allocated to the WBANs biomedical devices for communication. Following this, suppose that, out of the CH total channels in the network, $\mathcal{R}$ channels are dedicated to a WBAN; therefore, the first $\mathcal{R}$ channel is used by the AP to send the control signals, whereas the remaining $\mathcal{R}-1$ channels are used as data channels by biomedical devices with C_1 and C_2. The devices with C_1 are modeled as $\mathcal{D} = \{d_1, d_2, \ldots, d_D\}\ \forall\ d \in \mathcal{B}$, and the devices with C_2 are modeled as $\mathcal{G} = \{g_1, g_2, \ldots, g_G\}\ \forall\ g \in \mathcal{B}$. In a WBAN, only devices that have data to send are allocated channels, whereas others switch to sleep mode to save energy. Moreover, resources are allocated to the devices based on their priorities (φ) using the following equation:

$$\varphi = \frac{d_T}{\lambda_r\ \mathcal{P}_{\mathrm{len}}} \tag{1}$$

where d_T is the data type, λ_r is the rate at which the traffic is generated, and $\mathcal{P}_{\mathrm{len}}$ is the length of the packet.

D. MC-HYMAC Channel Access Mechanism

A channel access mechanism is used to divide the available WBAN channels between the WBAN devices and AP by regulating the channels used. The C_1 and C_2 channel access mechanisms are shown in Figs. 2 and 3, respectively.

1) Channel Mapping Mechanism: In this study, we propose a channel-mapping policy with which WBANs' biomedical devices access the channel based on the availability of the channels. Recall that, in a WBAN, the first $\mathcal{R}$ channel is used as the control channel, whereas the $\mathcal{R}-1$ channels are used as data channels. Therefore, we denote when a WBAN device gains access to the channel as 1 and when a WBAN device fails to access the channel as 0. Consequently,

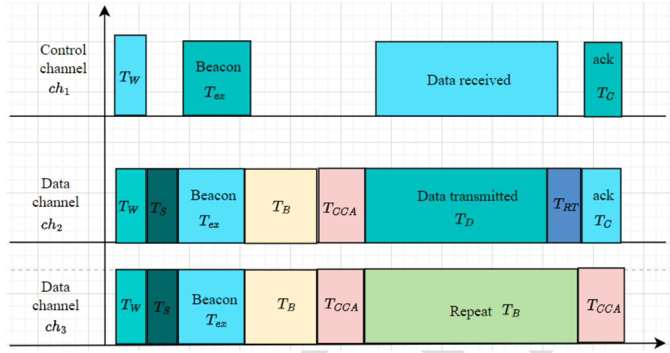

Fig. 2. Critical channel access mechanism.

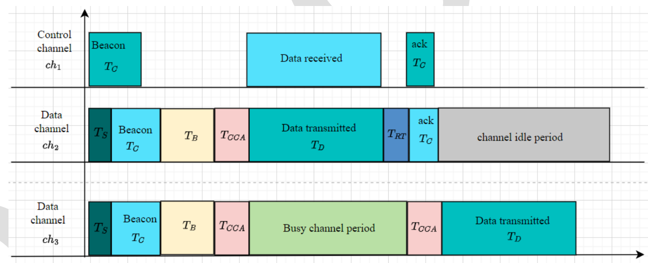

Fig. 3. Less-critical health packet channel access mechanism.

the channel-mapping matrix for accessing the channels is expressed as

$$a_{xy}^{n} = \begin{cases} 1, & \text{if } a_x \text{ accessed } \mathrm{ch}_y \\ 0, & \text{if } a_x \text{ failed to access } \mathrm{ch}_y \end{cases} \quad \forall\ x \in \mathcal{A}\ \forall\ y \in \mathrm{CH}. \tag{2}$$

Assuming that WBAN a_x and a_{x+1} simultaneously transmit their packets using the same frequency spectrum, interference would occur. The interference matrix is modeled as

$$I_{xy} = \begin{cases} 1, & \text{if } a_x \text{ interferes with } a_{x+1} \\ 0, & \text{if } a_x \text{ does not interfere with } a_{x+1} \end{cases} \quad \forall\ x \in \mathcal{A}. \tag{3}$$

In the proposed protocol, 1 denotes the possibility that two WBANs interfere with one another, and 0 denotes the possibility of no interference. However, the focus of this study is not on interference mitigation but on improving energy efficiency and throughput, prolonging the network lifetime, and minimizing delay and packet drop ratio.

2) Channel Selection Policy: In the proposed MC-HYMAC protocol, we assumed there are nine channels. Each channel is allocated a sequence number that ranges from 1 to 9. For each WBAN, before any communication commences, the AP checks the channels to determine free channels and creates a list of channel states. We assume that 11 in the list denotes that the referenced channel is available, whereas 00 denotes that the reference channel is unavailable, as shown in Fig. 4. Therefore, among the free channels, the AP selects a channel that is not occupied as the control channel, and all the devices listen to the channel for an incoming control command. It is important to note that other available channels can also be used as communication channels. The devices with C_2 health packets to transmit employ the CSMA/CA scheme to obtain contention allocations for the transmission of their health

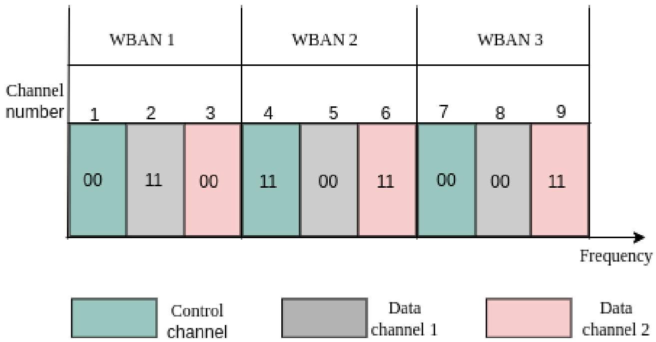

Fig. 4. Channel plane of multichannel in the MC-HYMAC protocol.

information (H-Info). H-Info does not contain the payload (i.e., actual intended health data). Consequently, after each channel is allocated to a device, the AP updates the channel list to prevent collisions [26].

E. Channel Modeling

In this section, we mathematically model the effect of the communication channel used to propagate generated health data from the patient's body to the AP. To achieve this, in the proposed system, we considered the effects of path loss, shadowing, fading, and power decay in a WBAN setting when modeling the WBAN communication channel. We consider the characteristics of WBAN communication channel path loss, which includes a distance-dependent path loss model with a path loss exponent of the considered communication environment and a small-scale fading effect modeled using a Rayleigh fading model. We modeled the path loss between a biomedical device and the AP using the empirical power decay law [26] as follows:

$$\mathcal{P}_d\ (dB) = \mathcal{P}_{d_0} + 10\ n \log_{10} \frac{d}{d_0} \tag{4}$$

where $\mathcal{P}_d$ represents the path, $\mathcal{P}_{d_0}$ denotes the distance, and n denotes the path-loss exponent. In general, the shadowing effect is introduced in the communication channel as a result of human body variation based on the environment. Therefore, combining shadowing with (4) gives a total path loss, which is modeled as

$$\mathcal{P}_t = \mathcal{P}_d + \mathcal{S}_f \tag{5}$$

where $\mathcal{S}_t$ represents the shadowing factor.

F. Back-Off Time Policy

To prolong the lifetime of the network and minimize energy consumption and delay, the benefits of IEEE 802.15.4, TDMA, and CSMA/CA protocols were combined in this study. We employed the IEEE 802.15.4 standard due to its potential to provide solutions for low-rate low-power wireless networks, such as WBANs. The TDMA scheme was used to allocate time slots to the devices. The CSMA/CA scheme is employed as a collision avoidance scheme to prevent repeated periodic collisions. After a collision occurs in the CAP, the devices perform a random back-off and contend to access the channel again. The back-off time determines the possibility of the devices gaining access to the channel. The shorter the back-off time, the higher the possibility of contending for a channel. However, a short back-off time increases the number of ReTs; therefore, an efficient back-off time scheme is required. The conventional back-off schemes adopt an exponential back-off method. In this case, if a device transmits when the channel is busy, it performs a random back-off process by selecting from interval (0, CW). The contention, denoted by CW($2^\delta - 1$), depends on the number of failed health packet transmissions, and the back-off exponent, denoted by δ, is set to a minimum of 3. For the first packet transmission attempt in a WBAN, the devices CW are set to a minimum value denoted by $\mathrm{CW_{MIN}}$, whereas, in the case of a failed transmission, CW is doubled to a maximum value denoted by $\mathrm{CW_{MAX}}(2^\delta \times \mathrm{CW_{MIN}})$. Therefore, the back-off time counter decreases when the channel is idle. Moreover, the devices back off immediately after transmission is sensed on the channel and then retransmit the packets again when the channel is idle until the back-off time is 0. Thus, the probability of collision is reduced. However, the devices would have to back off several times to achieve successful transmission. Consequently, we propose a new back-off time method for devices by setting a threshold for the contention value ($\mathrm{CW_{th}}$). Assume that the bit error rate is 0. Then, $\mathrm{CW_{th}}$ is expressed as

$$\mathrm{CW_{th}} = \frac{1}{2}\ (\mathrm{CW_{MIN}} + \mathrm{CW_{MAX}}). \tag{6}$$

A WBAN is configured to have a maximum value of $\delta = 5$ based on the IEEE 802.15.4 standard, which allows five back-off slots ranging from 0 to 31, i.e., 0–1, 0–15, 0–31, 0–31, and 0–31 [27]. This implies that the proposed back-off algorithm allows devices to contend five times for a channel. Suppose that the back-off time is uniformly distributed; then, the optimal time for accessing the channel is computed. For example, in the proposed protocol, δ is a random value ranging from $0 \geq 5$. Therefore, the back-off time slot and the mean value of the back-off time (Col) are expressed as

$$\mathrm{CW} = 2^\delta - 1 \tag{7}$$

$$E|\mathrm{Col}| = \frac{1}{a+1} \sum_{m=0}^{a} m. \tag{8}$$

Let us assume that, in a WBAN, we averaged three collisions, and then, a is determined

$$a = 2^\delta - 1 = 2^3 - 1 = 7. \tag{9}$$

Substituting (9) in (8) gives

$$E|\mathrm{Col}| = \frac{1}{a+1} \sum_{m=0}^{a} m = \frac{1}{7+1} \sum_{m=0}^{7} (0 + 1 + \ldots + 7) \tag{10}$$

$$\therefore\ E|\mathrm{Col}| = E(3) \approx 3. \tag{11}$$

With respect to the optimal value given in (8), $\mathrm{CW_{th}}$ is the corresponding back-off time slot. It is important to mention that the C_1 devices have less delay than the C_2 devices during transmission. The back-off scheme is presented in Algorithm 1.

Algorithm 1 Proposed MC-HYMAC Back-Off Time Scheme

Require: $\Rightarrow$ Biomedical devices that have data packet to transmit, back-off time-slot, δ, CW, CW_{MAX}, CW_{MIN}, CW_{th}
Ensure: $MIN_\delta = 3$, $MAX_\delta = 5$
1: locate the boundary slot
2: check channel state
3: **if** channel is idle **then**
4: perform clear channel assessment (CCA)
5: **else** channel state is busy
6: assign $\delta = 3$
7: back-off using CW_{MIN}
8: check channel state
9: **end if**
10: **if** channel state is still busy **then**
11: back-off using CW_{MAX}
12: assign $\delta = 5$
13: reset CW with a default value of 2
14: back-off again
15: wait for acknowledgment (ack)
16: **end if**
17: **if** channel state is idle **then**
18: decrease CW by 1 until it reaches 0
19: **end if**
20: **if** a_x access the channel ch_y successfully **then**
21: assign 1 using (2)
22: **else** set back-off time as CW_{MIN}
23: **end if**
24: **if** a_x failed to access ch_y **then**
25: assign 0 using (2)
26: go to step 2 and step 3
27: repeat until channel contention is successful
28: **end if**

G. Time-Slot Management Scheme

In the proposed MC-HYMAC protocol, we consider a heterogeneous-based WBAN system, in which WBAN biomedical devices have different priorities, data types, and data rates. The data rates of the devices usually vary from one device to another. For instance, a blood pressure sensor has 1.92 kb/s, an electrocardiography (ECG) sensor 192 kb/s, an electromyography (EMG) sensor 1536 kb/s, and a temperature sensor 1 kb/s. MEC allocates slots to the devices based on their data rate [28]. The MEC computes the number of slots to be allocated to each device and sends the details of the computations to the AP to avoid time-slot wastage

$$\zeta = \frac{D_r}{S_l} \tag{12}$$

$$\zeta/fr = \frac{\zeta}{50\ fr/\text{sec}} \tag{13}$$

$$S_{\text{num}} = \left\lceil \frac{\zeta}{\omega} \right\rceil \tag{14}$$

where D_r, ζ, S_l, ζ/fr, S_{num}, and ω denote the data rate, the number of symbols, the length of symbols, the number of symbols per frame, the number of slots, and the number of symbols per slot, respectively. Therefore, based on (12)–(14), the MEC assigns a time slot to each WBAN device through the AP. For example, two slots are allocated to an EEG sensor device, and one slot is allocated to the pulse rate device. Thereafter, the AP stores the time-slot values for each device in the form of an array. In the case of C_1 detection, the device with C_1 is assumed to have a higher priority based on (1), and the MEC assigns a time slot through the AP. We assume that the devices with C_2 have low priority and are assigned a CAP slot. The time-slot management scheme is presented in Algorithm 2.

Algorithm 2 Time-Slot Management Scheme

Require: $\{d_1, d_2, \ldots, d_D\}$ with C_1, $\{g_1, g_2, \ldots, g_G\}$ with C_2
Ensure: φ, D_r, S_r, ζ, ζ/fr, S_{num}, ω
1: **for** each d in C_1 **do**:
2: use (1) to calculate their φ
3: compute ζ, ζ/fr using (12) and (13)
4: compute an optimal time-slot using (14)
5: AP store time-slot values $\forall\ d \in \mathcal{D}$
6: **end for**
7: **for** each g in C_2 **do**
8: use (1) to calculate their φ
9: compute ζ, ζ/fr using (12) and (13)
10: compute an optimal time-slot using (14)
11: AP store time-slot values $\forall\ g \in \mathcal{G}$
12: **end for**

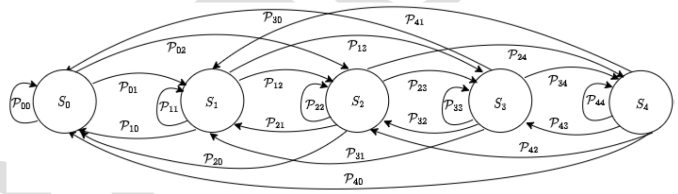

Fig. 5. Proposed MC-HYMAC state transition diagram.

IV. Markov Analysis

To determine the different states of biomedical devices, we propose a discrete-time finite-state Markov model. Based on this model, the following holds.

1) Control and data requests arrive independently at their respective destinations.
2) The devices have the capacity to store a finite number of health packets.
3) The biomedical devices cannot transmit health packets to the AP and receive control packets/signals from the AP, simultaneously.
4) In each WBAN, the devices in the network have different transmission probabilities based on their priority class.
5) The proposed system supports an ReT process and is regarded as a truncated Poisson distribution process.

The proposed Markov model has a finite number of states that denote different statuses of a device. The devices can change their status at any time in correspondence with the transitions between all possible states.

A. Discrete-Time Markov Chain

In the proposed model, the states of the devices are modeled, and all possible transitions and their probabilities are identified. The proposed Markov model with different transition probabilities and the transition states based on the time interval are presented in Figs. 5 and 6, respectively.

Based on the Markov property, the future states depend only on the present state and not on the past, that is, the past state does not have anything to do with how a state gets to its present

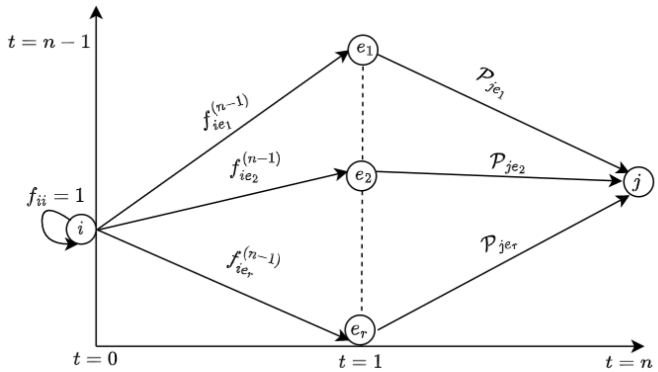

Fig. 6. Different transition states versus time intervals (t).

state or future predictions [29]. However, the past state could be helpful in determining future states more accurately.

Let the discrete time be represented as n such that $n = 0, 1, 2, 3, \ldots, \infty$. The arrival requests are modeled using the Bernoulli distribution process and are denoted as p, whereas the service time is represented as q and follows a geometric distribution. Thus, we represent the system state as X_n, where n is the number of transitions or time. Assuming that X_0 is the starting state of the system, X_0 can be assumed to be a given or random variable. As a consequence, the probability of transitioning from one state to another and the probability of arriving at state j after $n+1$ transitions $\forall$ past transitions are modeled in (15) and (16), respectively, while the state transition matrix is shown as

$$p_{ij} = \mathcal{P}(X_{n+1} = j | X_n = i) \quad \forall\ n = 0, 1, 2, 3, \ldots \tag{15}$$

$$p_{ij} = \mathcal{P}(X_{n+1} = j | X_n = i), \mathcal{P}(X_{n-1} = i - 1)$$
$$\mathcal{P}(X_{n-2} = i - 2), \ldots, X_0 \forall\ t \geq 0, i, j, i-1, \ldots \in \mathcal{S} \tag{16}$$

$$\mathcal{P}^{(n)} = \begin{array}{c} \\ 0 \\ 1 \\ 2 \\ 3 \\ . \\ . \\ . \end{array} \begin{array}{c} \begin{array}{ccccccc} 0 & 1 & 2 & 3 & . & . & . \end{array} \\ \begin{pmatrix} p_{00} & p_{01} & p_{02} & p_{03} & . & . & . \\ p_{10} & p_{11} & p_{12} & P_{13} & . & . & . \\ p_{20} & p_{21} & p_{22} & p_{23} & . & . & . \\ p_{30} & p_{31} & p_{32} & p_{33} & . & . & . \\ . & & & & & & \\ . & & & & & & \\ . & & & & & & \end{pmatrix} \end{array}. \tag{17}$$

In (15) and (16), p_{ij} denotes the discrete-time transition probability function where i is the source state and j is the final or destination state, while $\mathcal{S} = \{S_0^{C_1,C_2}, S_1^{C_1,C_2}, S_2^{C_1,C_2}, S_3^{C_1,C_2}, S_4^{C_1,C_2}\}$ is a set of finite sample spaces [30]. Here, $S_0^{C_1,C_2}$ is the sleep state, $S_1^{C_1,C_2}$ is the idle state, $S_2^{C_1,C_2}$ is the active state, $S_3^{C_1,C_2}$ is the receive state, and $S_4^{C_1,C_2}$ is the transmit state. Following this, the possible state of transitions are modeled as

$$\mathcal{P}_{00} = (1 - p)p \tag{18}$$
$$\mathcal{P}_{12} = (1 - q)p \tag{19}$$
$$\mathcal{P}_{21} = (1 - p)q \tag{20}$$
$$\mathcal{P}_{44} = (1 - p)(1 - q) + pq \tag{21}$$
$$f_{ij}^{t} = \mathcal{P}(X_{n+1} = j | X_0 = i). \tag{22}$$

where X_n denotes the final state after n iterations, and X_0 denotes the initial state. Moreover, there could be several transitioning states between i and j; thus, to find the final state j, the state before the final state must be identified first, which is modeled as

$$f_{ij}^{0} = \begin{cases} 1, & \text{if } i = j \\ 0, & \text{if } i \neq j \end{cases} \quad \forall\ i, j \in \mathcal{S}. \tag{23}$$

It is noteworthy to mention here that the number of transitions involved in getting to the $n - 1th$ state is insignificant and the system starts from the initial state X_0 and not the $n - 1th$ state. Following this, the probability of one step transition is modeled as

$$f_{ij}^{1} = \mathcal{P}_i j. \tag{24}$$

Therefore, the probability of going back to its own state is expressed as

$$f_{ii} = 1. \tag{25}$$

Based on the law of total probability, we modeled the n-step transition as

$$P(X_{n+1} = j | X_0 = i) = \mathcal{P}(X_n = j | X_0 = i) \quad \forall\ n = f_{ij}^{(n)}. \tag{26}$$

Moreover, the final state can be computed once a state $n - 1$ is reached, and this is also known as a recursion equation and is modeled as

$$f_{ij}^{t} = \sum_{e=i}^{r} f_{ie}^{(n-1)}\ \mathcal{P}_{ej} \quad \forall\ i, j\ \in \mathcal{S} \tag{27}$$

where the start or initial state is denoted by $X_0 = i$ after f_{ij}^{n} transition numbers. Consequently, the final state, denoted by $X_n = j$, can be calculated. The random initial state and the sum of all the transition states after the first state are modeled as

$$\mathcal{P}(X_n = j) = \sum_{i=1}^{r} \mathcal{P}(X_0 = i)\ f_{ij}^{n} \tag{28}$$

$$f_{ij}^{n} = \sum_{i=1}^{r} f_{i1}^{(n-1)}\ \mathcal{P}_{1j} \quad \forall\ i, j\ \in \mathcal{S}. \tag{29}$$

The probability of the transition state for n number of transitions is modeled as

$$f_{ij}^{n} = \sum_{e=1}^{r} f_{ie}^{(n-1)}\ \mathcal{P}_{ej} \quad \forall\ n = 0, 1, 2, 3, \ldots \tag{30}$$

Furthermore, to determine the probability that a Markov chain after n number of transitions with some initial state X_{iJ}^{n} converge to a steady state π_j can be modeled by taking the $\lim_{n\to\infty}$ of both sides in (30) to form (31) [24] as

$$\lim_{n\to\infty} f_{ij}^{n} = \lim_{n\to\infty} \sum_{e=1}^{r} f_{ie}^{(n-1)}\ \mathcal{P}_{ej} \quad \forall\ n = 0, 1, 2, 3, \ldots \tag{31}$$

Thus, from (31), we derive

$$\pi_j = \sum_{e=0}^{n} \pi_e\ \mathcal{P}_{ej} \quad \forall\ j \tag{32}$$

where π denotes the frequency of the transition from all possible states in the system to the final state j. From Fig. 3, it can be deduced that the steady-state transition probability of any state can be determined by changing j's value such that $\pi_1\mathcal{P}_{40}$, $\pi_2\mathcal{P}_{20}$, and $\pi_3\mathcal{P}_{10}$ are some of the transition frequencies to state 0, whereas the sum of the transition frequencies to state 0 is modeled as

$$\pi_0 = \sum_{u=0}^{n} \pi_u \ \mathcal{P}_{u0} \quad \forall\, n = 0, 1, 2, 3, \ldots \tag{33}$$

V. Performance Analysis of the Proposed System

In this section, we analyze the proposed system based on the energy consumption of the devices and the time spent by the devices to transmit health packets and delays. In addition, we presented an adaptive power control and allocation scheme. This is described in detail in the following.

A. Energy Consumption and Time Analysis

In practice, energy consumption is related to the device's behavior. A network with less busy traffic has lower energy consumption compared to a network with busy traffic. First, we present the total time spent when the channel is busy in a WBAN for devices with C_1 and C_2. We assume that the total numbers of devices that have C_1 and C_2 to transmit are denoted as k and h, respectively, $\forall\, k \in \mathcal{D}$ and $\forall\, h \in \mathcal{G}$, respectively. The average arrival times of devices with C_1 and C_2 are denoted by $T_{\text{avg}}^{C_1} = (1/\lambda)_T$ and $T_{\text{avg}}^{C_2} = (1/\lambda)_T$, respectively. We assume that, during the first CCA, the channel is busy when other devices transmit their health packets. Thus, let k_T represent the total number of health packets that are served when the channel is busy and is modeled [24] as

$$k_T = \frac{1}{1-\eta^{C_1}}. \tag{34}$$

The total time spent when the channel is busy (η^{C_1}) is modeled as

$$\eta^{C_1} = \frac{1}{\lambda_r}\left(T_W^{C_1} + T_B^{C_1} + T_S^{C_1} + 2T_{\text{RT}}^{C_1} + 2T_C^{C_1} + T_D^{C_1}\right) \tag{35}$$

where $T_W^{C_1}$, $T_B^{C_1}$, $T_S^{C_1}$, $T_{\text{RT}}^{C_1}$, $T_C^{C_1}$, and $T_D^{C_1}$ represent the wake-up time, the back-off time when the channel is busy, the startup time from $S_1^{C_1}$ to $S_4^{C_1}$, the random waiting time to receive an acknowledgment (ack) message, the control packet transmission time, and the data transmission time. The time interval in which $k-1$ devices spent in the channel is modeled as

$$\begin{aligned} T_{k-1}^{C_1} &= (k-1)T_k^{C_1} \\ &\quad \times\left(T_W^{C_1} + T_{\text{CCA}}^{C_1} + T_S^{C_1} + 2T_{\text{RT}}^{C_1} + 2T_C^{C_1} + T_D^{C_1}\right) \\ &\quad \times(1-\tau) \end{aligned} \tag{36}$$

where $T_k^{C_1}$ and τ denote the total time spent in the channel and the probability of packet loss, respectively. Consequently, the total time spent by a device with C_1 traffic in each state is modeled as

$$\mathcal{T}_t^{C_1} = \mathcal{T}_{S_0}^{C_1} + \mathcal{T}_{S_1}^{C_1} + \mathcal{T}_{S_2}^{C_1} + \mathcal{T}_{S_3}^{C_1} + \mathcal{T}_{S_4}^{C_1} \quad \forall\, d \in \mathcal{D} \tag{37}$$

where $\mathcal{T}_{S_0}^{C_1}$ is the time spent in the sleep state, which includes the wake-up time; $\mathcal{T}_{S_1}^{C_1}$ is the time spent in the idle state, which includes the random waiting time; $\mathcal{T}_{S_2}^{C_1}$ is the time spent in the active state, which includes the back-off time and the CCA time; $\mathcal{T}_{S_3}^{C_1}$ is the time spent in the receiving state for receiving control packets from the MEC through the AP; and $\mathcal{T}_{S_4}^{C_1}$ is the time spent in the transmission state, which includes the startup time, the data transmission time, the beacon time, and the acknowledgment time. Thus, the total power spent by a device in each state is modeled as

$$\begin{aligned} \mathcal{P}_S^{C_1} &= \mathcal{P}_{S_0}^{C_1}\left(\mathcal{T}_{S_0}^{C_1}\right) + \mathcal{P}_{S_1}^{C_1}\left(\mathcal{T}_{S_1}^{C_1}\right) + \mathcal{P}_{S_2}^{C_1}\left(\mathcal{T}_{S_2}^{C_1}\right) \\ &\quad + \mathcal{P}_{S_3}^{C_1}\left(\mathcal{T}_{S_3}^{C_1}\right) + \mathcal{P}_{S_4}^{C_1}\left(\mathcal{T}_{S_4}^{C_1}\right) \quad \forall\, d \in \mathcal{D}. \end{aligned} \tag{38}$$

The average energy consumed by devices with C_1 $(\mathcal{E}^{C_1})$ is modeled as

$$\begin{aligned} \mathcal{E}^{C_1} &= \Big(\mathcal{P}_{S_1}^{C_1}\Big(\lambda_T - \Big(T_W^{C_1} + T_S^{C_1} + 2T_{\text{RT}}^{C_1} + 2T_C^{C_1} + T_{\text{CCA}}^{C_1} \\ &\quad + T_D^{C_1} + T_{\text{beacon}}^{C_1}\phi^{C_1}\Big)\Big) + \mathcal{P}_{S_4}^{C_1} T_W^{C_1} + \mathcal{P}_{S_3}^{C_1} T_{\text{beacon}}^{C_1}\phi^{C_1} \\ &\quad + \mathcal{P}_{S_3}^{C_1}\left(T_S^{C_1} + 2T_{\text{RT}}^{C_1} + 2T_C^{C_1}\right) + \mathcal{P}_{\text{CCA}}^{C_1} T_{\text{CCA}}^{C_1} N_{\text{CCA}}^{C_1}\Big) \Big/ \lambda_T \\ &\quad + \mathcal{E}_A^{C_1}\left(\phi^{C_1} T_{\text{beacon}}^{C_1} + T_B^{C_1}\right) \end{aligned} \tag{39}$$

where $\mathcal{P}_{S_1}^{C_1}$, $\mathcal{P}_{S_3}^{C_1}$, $\mathcal{P}_{S_4}^{C_1}$, and $\mathcal{P}_{\text{CCA}}^{C_1}$ represent the power consumption in the idle state, the receive state, the transmission state, and CCA, respectively. In addition, ϕ^{C_1}, $T_{\text{beacon}}^{C_1}$, $T_{\text{CCA}}^{C_1}$, λ_T, and $N_{\text{CCA}}^{C_1}$ represent the probability that the channel is busy, the time taken to transmit a beacon message, the CCA transmission time, the average arrival time, and the total number of CCA until the health packet is transmitted successfully to the destination, respectively. The CCA was assumed to have a maximum number of 2.

For the devices with C_2, we denoted the number of health packets that are served when the channel is busy as h_T and is modeled as

$$h_T = \frac{1}{1-\eta^{C_2}}. \tag{40}$$

Therefore, the total time spent by the C_2 devices when the channel is busy η^{C_2} is modeled as

$$\begin{aligned} \eta^{C_2} &= \frac{1}{\lambda_T}\Big(T_S^{C_2} + T_{\text{beacon}}^{C_2} + 2T_{\text{RT}}^{C_2} + 2T_C^{C_2} \\ &\quad + T_{\text{CCA}}^{C_2} + T_D^{C_2} + T_{\text{ack}}^{C_2} + T_p^{C_2} + T_{\text{avgb}}^{C_2}\phi^{C_2}\Big) \end{aligned} \tag{41}$$

where $T_p^{C_2}$ and $T_{\text{avgb}}^{C_2}$ are the propagation and average arrival times between the two beacons, respectively. Following this, the total time and power spent by a device with C_2 traffic in each state are modeled and (43) as

$$\mathcal{T}_t^{C_2} = \mathcal{T}_{S_0}^{C_2} + \mathcal{T}_{S_1}^{C_2} + \mathcal{T}_{S_2}^{C_2} + \mathcal{T}_{S_3}^{C_2} + \mathcal{T}_{S_4}^{C_2} \quad \forall\, g \in \mathcal{G} \tag{42}$$

$$\begin{aligned} \mathcal{P}_S^{C_2} &= \mathcal{P}_{S_0}^{C_2}\left(\mathcal{T}_{S_0}^{C_2}\right) + \mathcal{P}_{S_1}^{C_2}\left(\mathcal{T}_{S_1}^{C_2}\right) \\ &\quad + \mathcal{P}_{S_2}^{C_2}\left(\mathcal{T}_{S_2}^{C_2}\right) + \mathcal{P}_{S_3}^{C_2}\left(\mathcal{T}_{S_3}^{C_2}\right) + \mathcal{P}_{S_4}^{C_2}\left(\mathcal{T}_{S_4}^{C_2}\right) \quad \forall\, g \in \mathcal{G}. \end{aligned} \tag{43}$$

The average energy consumed by the devices with C_2 ($\mathcal{E}^{C_2}$) in the receive state, transmit state, and during the back-off period is modeled as

$$\mathcal{E}^{C_2} = \mathcal{E}^{C_2}_E + \mathcal{E}^{C_2}_B + \mathcal{E}^{C_2}_{S_3} + \mathcal{E}^{C_2}_{S_4} \tag{44}$$

where $\mathcal{E}^{C_2}_E$ denotes the energy consumed during the idle state, startup, back-off, CCA, data transmission, and average beacon arrival time. $\mathcal{E}^{C_2}_B$ is the energy spent during back-off, $\mathcal{E}^{C_2}_{S_3}$ is the energy spent in the receiving state, and $\mathcal{E}^{C_2}_{S_4}$ is the energy consumed in the transmission state. Therefore, $\mathcal{E}^{C_2}_E$, $\mathcal{E}^{C_2}_B$, $\mathcal{E}^{C_2}_{S_3}$, and $\mathcal{E}^{C_2}_{S_4}$ are expressed as

$$\mathcal{E}^{C_2}_E = \mathcal{P}^{C_2}_{S_1}\Big(\lambda_T - \Big(T^{C_2}_S + T^{C_2}_{\text{beacon}} + T^{C_2}_{\text{CCA}} + T^{C_2}_D + T^{C_2}_{\text{ack}} + T^{C_2}_{\text{avgb}}\phi^{C_2}\Big) \tag{45}$$

$$\mathcal{E}^{C_2}_{Wb} = \mathcal{P}^{C_2}_{S_3}\Big(T^{C_2}_{\text{avgb}}\rho^{C_2}\Big) \tag{46}$$

$$\mathcal{E}^{C_2}_{S_3} = \mathcal{P}^{C_2}_{S_3}\Big(T^{C_2}_S + 2T^{C_2}_C + 2T^{C_2}_p\Big) \tag{47}$$

$$\mathcal{E}^{C_2}_{S_4} = \mathcal{P}^{C_2}_{S_4}\Big(T^{C_2}_D\Big). \tag{48}$$

From (45) to (48), we derive (49), which is the average energy consumed by the C_2 devices

$$\mathcal{E}^{C_2} = \Big(\mathcal{P}^{C_2}_{S_1}\Big(\lambda_T - \Big(T^{C_2}_S + T^{C_2}_{\text{beacon}} + T^{C_2}_{\text{CCA}} + T^{C_2}_D + T^{C_2}_{\text{ack}} + T^{C_2}_{\text{avgb}}\phi^{C_1}\Big)\Big) + \Big(\mathcal{P}^{C_2}_{S_3}T^{C_2}_{\text{avgb}}\Big) + \Big(\mathcal{P}^{C_2}_{S_3}T^{C_2}_{\text{beacon}}T_{\text{ex}}\phi^{C_2}\Big) + \Big(\mathcal{P}^{C_2}_{S_3}T^{C_2}_S + 2T^{C_2}_p + 2T^{C_2}_C\Big) + (\mathcal{P}^{C_2}_{S_4}T^{C_2}_D)\Big)\Big/\lambda_T \tag{49}$$

where T_{ex} is the extra time spent transmitting the beacon. Furthermore, we optimize the time spent by the devices in each state by setting a time constraint (t) to assign different time to a biomedical device in the different states, i.e., $\mathcal{S} = \{S^{C_1,C_2}_0, S^{C_1,C_2}_1, S^{C_1,C_2}_2, S^{C_1,C_2}_3, S^{C_1,C_2}_4\}$ using the following equation:

$$t_n = t_{S_0} + t_{S_1} + t_{S_2} + t_{S_3} + t_{S_4} = 1 \tag{50}$$

where $t_{S_0}, t_{S_1}, t_{S_2}, t_{S_3}$, and t_{S_4} are the total time spent during the sleep, idle, active, receive, and transmit states, respectively. The power spent by the devices in each state is optimized by computing a power resource allocation solution to optimally assign power to devices. Therefore, we present an adaptive-based power–resource allocation scheme in Algorithm 3.

B. Delay Analysis

We employ an M/M/1 queuing model [29] to formulate the average delay ($D^{C_1}_{\text{avg}}$) experienced during C_1 transmission. The $D^{C_1}_{\text{avg}}$ is modeled as

$$D^{C_1}_{\text{avg}} = \phi T^{C_1}_B + \frac{\lambda_r^2 Var(\mathcal{S})}{2(1-\rho)} + \Big(T^{C_1}_{\text{beacon}} + T^{C_1}_W + \Big(T^{C_1}_D + 2T^{C_1}_{\text{RT}} + 2T^{C_1}_C\Big)\Big) \tag{51}$$

where the utilization is $\rho = (\lambda_r/\mu)$, the mean service time distribution (S) is $\mu = (1/S)$, and the variance of the service time is Var(S). For the C_2 transmission, the average delay is modeled in (52) as

$$D^{C_2}_{\text{avg}} = \phi\Big(T^{C_2}_B + T^{C_2}_{\text{CAP}} + T^{C_2}_{\text{CFP}}\Big) + \Big(T^{C_2}_D + 2T^{C_2}_{\text{RT}} + 2T^{C_2}_C\Big). \tag{52}$$

Algorithm 3 Adaptive Power Control Scheme

Require: $\mathcal{D} = \{d_1, d_2, \ldots, d_D\}$, $\mathcal{G} = \{g_1, g_2, \ldots, g_G\}$, $t_n = \{t_1, t_2, t_3, t_4\}$
Ensure: $\mathcal{P}^{C_1,C_2}_{S_0}, \mathcal{P}^{C_1,C_2}_{S_1}, \mathcal{P}^{C_1,C_2}_{S_2}, \mathcal{P}^{C_1,C_2}_{S_3}, \mathcal{P}^{C_1,C_2}_{S_4}\}$, $\mathcal{P}^{C_1,C_2}_{S_2}$ is the power spent during the active state
for each d with C_1 **do**:
  set a time constraint using (45)
  find an optimal power allocation for $S^{C_1}_0$ s.t. $0 \le t_{S_0} \le 1$ and $\mathcal{P}_{min} \le \mathcal{P}^{C_1}_{S_0} \le \mathcal{P}_{max}, \forall\, d \in S^{C_1}_0$
  calculate an optimal power allocation for $S^{C_1}_1$ s.t. $0 \le t_{S_1} \le 1$ and $\mathcal{P}_{min} \le \mathcal{P}^{C_1}_{S_1} \le \mathcal{P}_{max}, \forall\, d \in S^{C_1}_1$
  find an optimal power allocation for $S^{C_1}_2$ s.t. $0 \le t_{S_2} \le 1$ and $\mathcal{P}_{min} \le \mathcal{P}^{C_1}_{S_2} \le \mathcal{P}_{max}, \forall\, d \in S^{C_1}_2$
  determine an optimal power allocation for $S^{C_1}_3$ s.t. $0 \le t_{S_3} \le 1$ and $\mathcal{P}_{min} \le \mathcal{P}^{C_1}_{S_3} \le \mathcal{P}_{max}, \forall\, d \in S^{C_1}_3$
  calculate an optimal power allocation for $S^{C_1}_4$ s.t. $0 \le t_{S_4} \le 1$ and $\mathcal{P}_{min} \le \mathcal{P}^{C_1}_{S_4} \le \mathcal{P}_{max}, \forall\, d \in S^{C_1}_4$
end for
for each g with C_2 **do**:
  set a time constraint using (45)
  find an optimal power allocation for $S^{C_2}_0$ s.t. $0 \le t_{S_0} \le 1$ and $\mathcal{P}_{min} \le \mathcal{P}^{C_2}_{S_0} \le \mathcal{P}_{max}, \forall\, d \in S^{C_2}_0$
  determine an optimal power allocation for $S^{C_2}_1$ s.t. $0 \le t_{S_1} \le 1$ and $\mathcal{P}_{min} \le \mathcal{P}^{C_2}_{S_1} \le \mathcal{P}_{max}, \forall\, d \in S^{C_2}_1$
  calculate an optimal power allocation for $S^{C_2}_2$ s.t. $0 \le t_{S_2} \le 1$ and $\mathcal{P}_{min} \le \mathcal{P}^{C_2}_{S_2} \le \mathcal{P}_{max}, \forall\, d \in S^{C_2}_2$
  find an optimal power allocation for $S^{C_2}_3$ s.t. $0 \le t_{S_3} \le 1$ and $\mathcal{P}_{min} \le \mathcal{P}^{C_2}_{S_3} \le \mathcal{P}_{max}, \forall\, d \in S^{C_2}_3$
  get an optimal power allocation for $S^{C_2}_4$ s.t. $0 \le t_{S_4} \le 1$ and $\mathcal{P}_{min} \le \mathcal{P}^{C_2}_{S_4} \le \mathcal{P}_{max}, \forall\, d \in S^{C_2}_4$
end for

VI. Protocol Description

Several standards, including IEEE 802.15.6 [31], ESTI SmartBAN [32], and IEEE 802.15.4 [33], have been used to cater to different WBAN requirements and applications. These standards were designed to address specific requirements and use cases of wireless communication systems. The IEEE 802.15.6 focuses on WBANs, whereas ETSI SmartBAN is tailored for medical device communication. The IEEE 802.15.4 standard was designed for devices that require low-cost and low-data-rate connectivity. Among these three wireless communication standards, IEEE 802.15.4 is regarded as the most fully developed short-range standard with a wide range of applications for WBANs in health-care [34]. Moreover, to address the constraints posed by energy scarcity and processing power of biomedical devices, the IEEE 802.15.4 standard incorporates suitable physical and MAC layers for battery-operated devices. In addition, IEEE 802.15.4 supports the design of mechanisms such as time-slotted access and multichannel communication to improve the performance of WBAN [34].

In this work, based on the IEEE 802.15.4 [35] standard for WBAN, we proposed a new hybrid CSMA/CA and TDMA protocol different from [11], [15], [16], [17], [18], [19], [20], [21], [22], [36], [37], [38], [39], [40], and [41] to address different shortcomings, such as channel utilization issue, energy consumption issue, time slot and energy wastage issues, and delay issue, in the existing MAC protocols. The proposed protocol consists of four phases, namely, the contention access phase (CAP), the contention free phase (CFP), the extended access phase (EAP), and the inactive phase (IP). We introduced an EAP for the transmission of C_1. In addition, the proposed MC-HYMAC protocol operates in beacon-enabled mode, and we assumed that the major operation of the devices is to transmit their health packets to the AP. The superframe structure of the system starts with a beacon message from the AP; it has the address of the AP and the devices at the start and end of the phases.

At the beginning of a cycle, all devices in the network are assumed to be in the sleep state, waiting for a ready-to-receive (RTR) beacon message from the AP. We employ a wake-up radio to switch the devices on and off [42], [43] to enhance the energy efficiency of the system. The wake-up radio operates by switching on the main radio of the device when an incoming signal is sensed. Consequently, the devices promptly switched to the active state. During the CAP, the devices with C_2 that has health packets to transmit would contend to transmit their H-Info by applying the CSMA/CA scheme using their own CW. Every successfully contended H-Info has its own unique information, including the device ID that will be used during transmission. After the AP successfully receives the H-Info, a total acknowledgment (T-ack) message is sent. The T-ack message has the channel number allocated to the devices, the transmission order, and the GTS. It is sent at the end of the CAP instead of after each received C_2 to reduce the device waiting time delay and save energy.

When C_1 is generated, the device with C_1 sends an emergency information (E-Info) to the AP without any contention. The AP sends a T-ack message to the devices upon reception of the E-Info. The T-ack message has a transmission order and specific time slot that would be used during the EAP. The transmission of E-Info is performed using the EAP, so as not to interfere with the C_2 transmission. The superframe structure of the proposed protocol is presented in Fig. 7, where the beacon interval is $\mathrm{BI} = \mathrm{aBaseSuperframDuration} \times 2^{\mathrm{BO}}$ and the supframe duration is $\mathrm{SD} = \mathrm{BaseSuperframDuration} \times 2^{\mathrm{SO}}$. The operation of the proposed MC-HYMAC scheme is presented in Algorithm 4.

A queuing order Q_{order} state is introduced for efficient transmission and energy conservation. In this state, only the synchronous clock of the devices is allowed to work, whereas all other operations are stopped. The devices were assumed to enter the Q_{order} state based on their priority. An M/M/1

Algorithm 4 Proposed MC-HYMAC Operation Scheme

Require: C_1 and C_2 ready to transmit
Ensure: back-off time, S_{num}, CW_{th}
1: **for** the beginning of a cycle **do**
2: AP send RTR to the devices
3: C_2 devices start the CAP to send H-Info
4: use the Ch_1 for the CAP
5: apply the CSMA/CA scheme
6: **for** C_2 successful contended devices (σ) **do**
7: AP send a T-ack at the end of the CAP
8: check the channel status using algorithm 1
9: assign a Q_{order} $\forall\ \sigma \in \mathcal{G}$
10: allocate time-slot in the CFP using algorithm 2
11: transmit C_2 to the AP and send an end beacon
12: AP send an O-ack $\forall$ successfully received C_2
13: **end for**
14: **if** a C_1 is detected **then**
15: send E-Info to the AP using the TDMA scheme
16: AP transmit T-ack
17: check the channel status using algorithm 1
18: assign a Q_{order} $\forall\ d \in \mathcal{D}$
19: allocate a time-slot in the EAP using algorithm 2
20: transmit C_1 to the AP and send an end beacon
21: AP send an O-ack $\forall$ successfully received C_1
22: **else**
23: go back to step 3
24: **end if**
25: **for** each failed transmission **do**
26: remain in the Q_{order} state until the end of all the transmission process
27: send a ReT beacon to the AP
28: repeat step 8 to 11 until an O-ack is received
29: **end for**
30: **end for**

queuing model is employed by using the first-in–first-out (F/I/F/O) approach to model the arrival and service rates of the devices. Devices in the Q_{order} state can only be activated to another active state with the device ID and their active beacons. In addition, the devices transmit their packets using a TDMA scheme, and at the end of each transmission, they send an end beacon to the AP. Upon receiving the health packets, the AP sends a beacon message to the devices that contain an order acknowledgment (O-ack) to activate the next device with an ID and active beacon. Then, we assume that the next device in the Q_{order} starts its transmission as soon as an O-ack message is received, whereas no O-ack message is sent in the case of a failed health packet transmission. In this case, the devices involved would remain in the Q_{oder} state until the end of the transmission process, before sending an ReT beacon to prepare the AP for the ReT process to save energy. The AP transmits an O-ack message after receiving an end beacon from the device.

VII. Simulation Results

The simulation results of the proposed MC-HYMAC protocol are presented in this section. We evaluated the performance of the proposed MC-HYMAC through extensive computer simulations using MATLAB and compared it with existing protocols, such as MSS-IEEE 802.15.4, IEEE 802.15.4, MG-HYMAC, and HyMAC. The network consisted of $\mathcal{A}$ WBANs

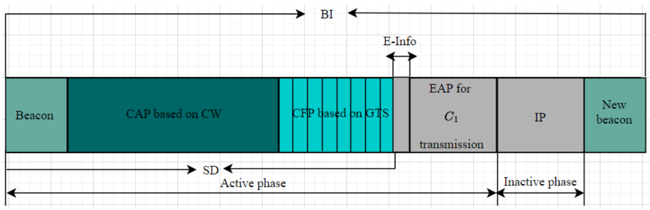

Fig. 7. Proposed MC-HYMAC superframe structure.

TABLE I
SIMULATION PARAMETERS

Parameter	Setting
Number of devices	10
Data rate	250 Kbps
BI	15360 symbols
Beacon order	4
Superframe order	3
back-off period	20 symbols
SD	7860 symbols
ack packet size	104 bits
CW_{MIN}	32
$CWMAX$	256
CCA	8 symbols
DIFS	$40 * 16e^{-6}\mu$
SIFS	$12 * 16e^{-6}\mu$
ω	60 symbols
Payload	624 bits
Receiving power	1.8 W
Receiving voltage	0.9 V
Transmission voltage	1.5 V
Transmission power	131.5 W
Distance between devices and AP	2 - 10 m

and CH channels. In each WBAN, we assume two types of devices: $\mathcal{D}$ and $\mathcal{G}$, where $\mathcal{D}$ devices generate C_1, whereas $\mathcal{G}$ devices generate C_2. Also, we assumed a total number of nine channels for the three WBANs considered. Each WBAN consisted of one AP and ten devices. In addition, we assumed that, in each WBAN, three channels were deployed for intra-WBAN communication, that is, communication between the devices and the AP. The devices communicate with the AP by using a single-hop topology. The same unit back-off duration of 20 symbols as the IEEE 802.15.4 standard was used, that is, 320 μs for 2.4 GHz. The simulation parameters employed [24] are listed in Table I. For evaluation and validation sakes, the proposed MC-HYMAC protocol was compared with some existing protocols, such as MSS-IEEE 802.15.4, MG-HYMAC, IEEE 802.15.4, and HyMAC, using standard performance metrics, such as energy efficiency, delay, packet drop and packet received (throughput) ratio, and the devices lifetime.

A. Energy Consumption Impact on Number of Devices

We investigate the impact of energy consumption on the number of devices as the devices were varied from 1 to 10 in this section. The proposed MC-HYMAC was compared and evaluated with existing protocols, such as MSS-IEEE 802.15.4, MG-HYMAC, IEEE 802.15.4, and HyMAC, in a transmission cycle. To achieve this, the proposed MC-HYMAC and existing protocols were configured with ten devices in a WBAN system. For the proposed MC-HYMAC

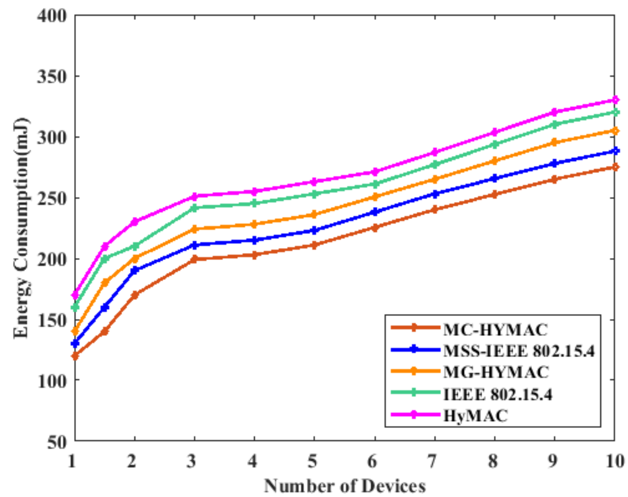

Fig. 8. Energy consumption against the number of devices.

protocol, we assume that $\mathcal{D}$ devices $= 4$ and $\mathcal{G}$ devices $= 6$. However, we assume that not all devices have data packets to be sent in each cycle. Therefore, the MC-HYMAC algorithms were enabled during the simulations and disabled during the simulations of existing protocols.

Also, the MC-HYMAC and other existing protocols are set to a transmission probability of 0.8, and we present the results of the simulations in Fig. 8.

We observed from Fig. 8 that, as the number of devices varies from 1 to 10, more energy was dissipated. However, because of the proposed algorithms and the different energy resource management strategies considered, the devices saved a reasonable amount of energy during their operations. In addition, it was observed that the MC-HYMAC protocol performed better than the existing protocols; for instance, when the devices were set to 6, approximately 225.5 mJ of energy was consumed, whereas, for MSS-IEEE 802.15.4, MG-HYMAC, IEEE 802.15.4, and HyMAC protocols, approximately 238, 250.5, 261, and 271 mJ, respectively, were consumed.

Consequently, the MC-HYMAC protocol consumed a lower amount of energy compared to MSS-IEEE 802.15.4, MG-HYMAC, IEEE 802.15.4, and HyMAC, with energy reductions of approximately 6%, 11%, 16%, and 20%, respectively. The improvement is due to the fact that the proposed MC-HYMAC protocol employs a multichannel concept for communication between the devices and the AP, and also employs a channel utilization mechanism to efficiently utilize the channels. The mechanism helped the devices know when to transmit their health packets and, therefore, reduce energy consumption, delay, and collisions. Also, we proposed an adaptive power control scheme, a dynamic time-slot management scheme, and a back-off period policy for the efficient utilization of the proposed channels.

B. Energy Consumption Impact on Transmission Probability

The performance of the proposed MC-HYMAC protocol was compared and evaluated using the existing protocols. For this experiment, we investigated the impact of energy

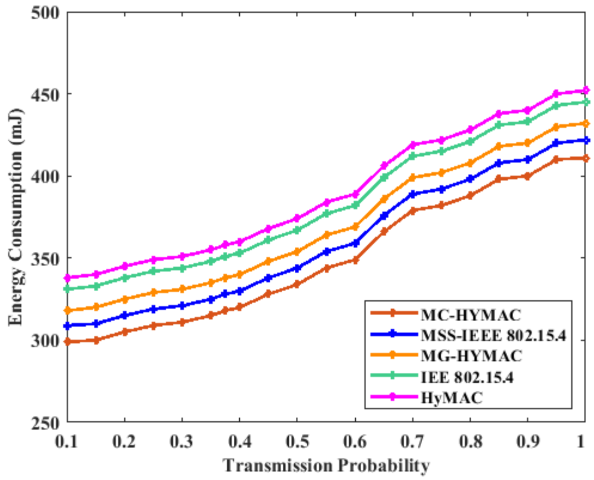

Fig. 9. Average energy consumption against transmission probability.

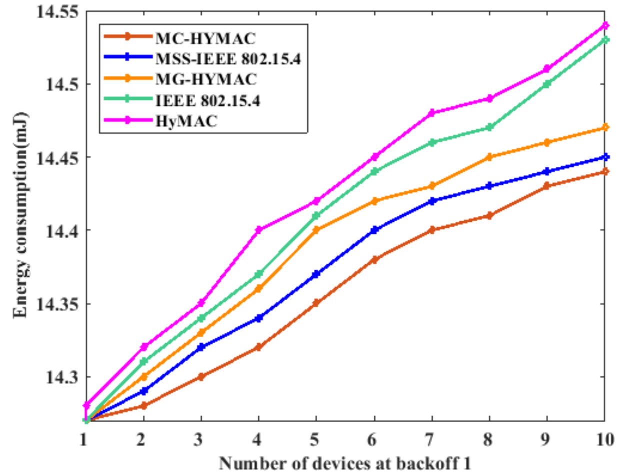

Fig. 10. Average energy consumption against the number of devices at back-off 1.

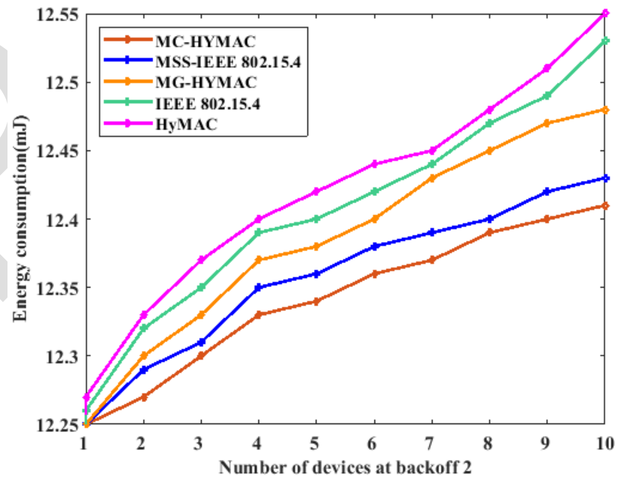

Fig. 11. Average energy consumption against the number of devices at back-off 2.

consumption on the transmission probability of devices in a WBAN system. Consequently, we configured the proposed MC-HYMAC, MSS-IEEE 802.15.4, MG-HYMAC, IEEE 802.15.4, and HyMAC protocols by varying the number of devices from 1 to 10. Therefore, we set $\mathcal{D}$ devices = 4 and $\mathcal{G}$ devices = 6. Also, we performed different experiments, and the outcomes of the experiments are shown in Fig. 9.

From Fig. 9, we noticed that the higher the transmission probability, the higher the amount of energy consumed. However, MC-HYMAC is advantageous compared to the other protocols because of the different energy management strategies that were considered, for example, the sending of a T-ack at the end of the CAP rather than sending the T-ack after each received H-Info or E-Info to save energy. Consequently, when the transmission probability of the system was set to 0.8, the MC-HYMAC protocol achieved significant energy reductions of approximately 2%, 5%, 9%, and 10% over the MSS-IEEE 802.15.4, MG-HYMAC, IEEE 802.15.4, and HyMAC protocols, respectively. These improvements could be attributed to the fact that the devices and the AP used separate channels for their communications, thereby reducing energy consumption and delay, enhancing transmission efficiency, increasing the packet delivery ratio, and improving the lifetime of the WBAN network. In addition, the improvement was also a result of the proposed adaptive power allocation scheme, the dynamic time-slot allocation scheme, and the back-off period policy that was employed to prevent energy wastage and time-slot wastage, and improve the lifetime of the network.

C. Energy Consumption on the Number of Devices Based on Different Back-Off Periods

In this section, we compare and evaluate the proposed MC-HYMAC protocol with the existing MSS-IEEE 802.15.4, MG-HYMAC, IEEE 802.15.4, and HyMAC protocols based on the energy consumption of the devices at different number of back-off periods. For the experiments, we varied the number of devices from 1 to 10, and configured the $\mathcal{D}$ devices as 4 and the $\mathcal{G}$ devices as 6. The experimental results are shown in Figs. 10–12. From Figs. 10 to 12, it can be observed that the proposed MC-HYMAC protocol consumed less energy compared to other existing protocols. For example, in Fig. 10, when the devices were set to 7, the MC-HYMAC protocol consumed about 14.40 mJ amount of energy compared to other existing protocols, such as MSS-IEEE 802.15.4 with about 14.42 mJ, MG-HYMAC with about 14.43 mJ, IEEE 802.15.4 with about 14.46 mJ, and HyMAC with 14.48 mJ. The improvement is due to the proposed back-off period policy, which was able to reduce the probability of collisions, thereby conserving energy and minimizing delay. In addition, the proposed adaptive energy control scheme helped allocate optimal energy resources to the devices, thereby prolonging the lifetime of the devices.

Furthermore, for the proposed MC-HYMAC protocol, we investigated the amount of energy consumed by the devices based on the number of back-off attempts during the busy channel period. The results of the simulation experiments are presented in Fig. 13.

From Fig. 13, we observed that, as we increased the number of devices, the amount of energy consumption also increased. However, we noticed a slight energy decrease in the second and third back-off attempts compared with the first attempt. For instance, when the devices were set to 9, for the first attempt, the devices consumed approximately 4.55 mJ, and

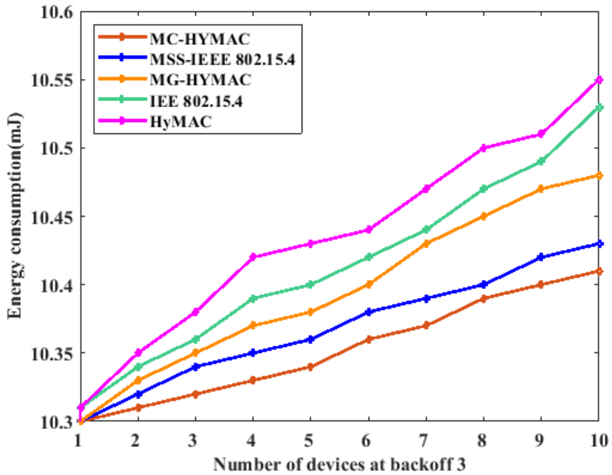

Fig. 12. Average energy consumption against the number of devices at back-off 3.

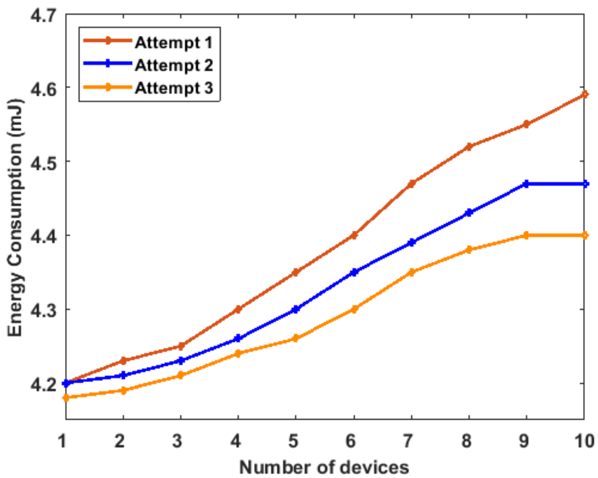

Fig. 13. Average energy consumption of the proposed MC-HYMAC protocol based on different back-off attempts during the channel busy period.

for the second attempt, approximately 4.57 mJ of energy was consumed, while approximately 4.40 mJ of energy was consumed for the third attempt. This improvement is a result of the multichannel concept proposed for communication between the AP and devices. Also, the improvement could be attributed to the efficient channel access mechanism and the back-off time scheme that were employed to identify the channel busy and channel idle periods for the efficient utilization of the channels.

D. Delay Impact on the Number of Devices Based on Different Back-Off Periods

In this section, the average packet delivery delay with respect to the number of devices based on different back-off periods in a WBAN system is investigated. To achieve this, the proposed MC-HYMAC protocol and the existing MSS-IEEE 802.15.4, MG-HYMAC, IEEE 802.15.4, and HyMAC protocols were configured with ten devices. For the MC-HYMAC protocol, when the total number of devices is 10, $\mathcal{D}$ devices = 4, and $\mathcal{G}$ devices = 6. Consequently, different experiments were performed, and the results of the experiments are presented in Figs. 14–16. From Fig. 14, we can deduce

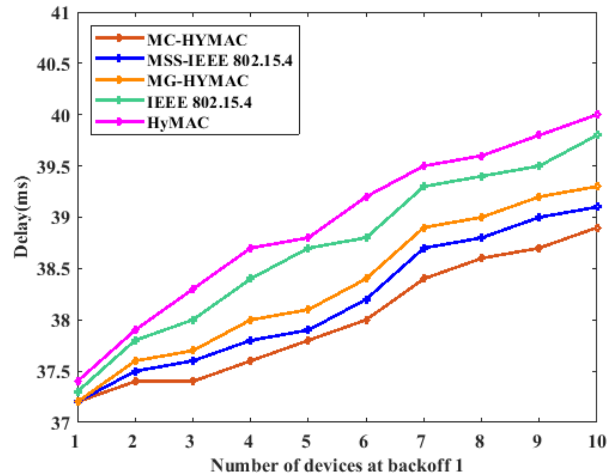

Fig. 14. Average delay versus the number of devices at back-off 1.

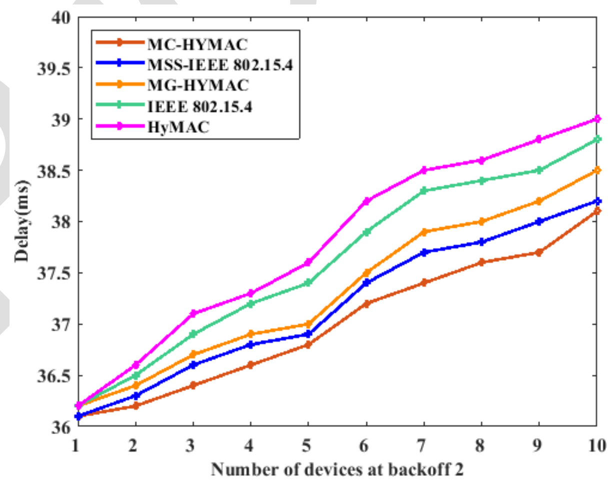

Fig. 15. Average delay versus the number of devices at back-off 2.

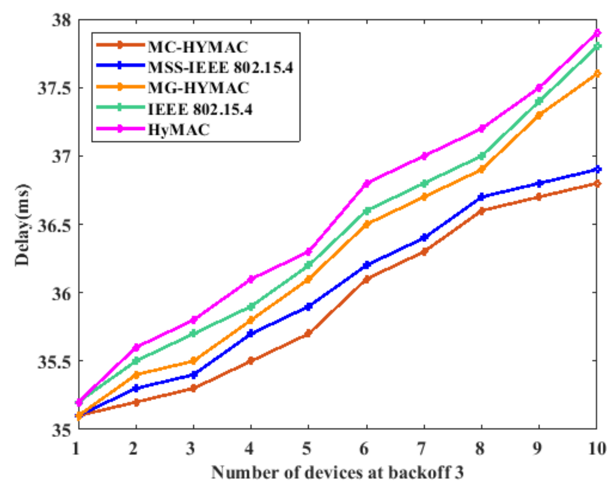

Fig. 16. Average delay versus the number of devices at back-off 3.

that, as we vary the number of devices participating in the data transmission process from 1 to 10, the delay experienced increases.

In general, the average delay of a system can be determined from the packet generation time interval to when the packets are successfully received at the side of the AP. However, during the transmission process, devices can experience

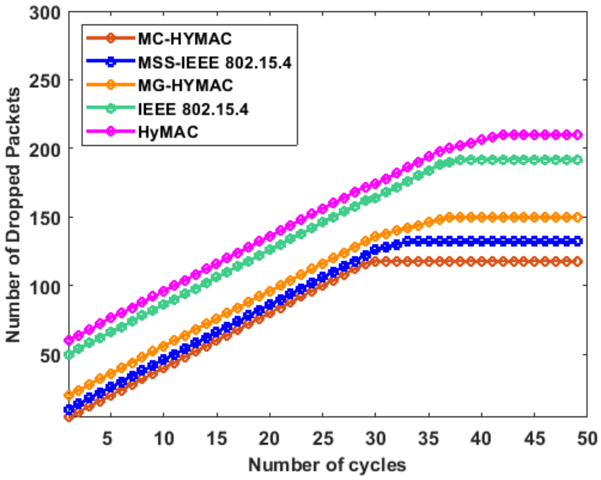

Fig. 17. Number of packets dropped based on the number of cycles.

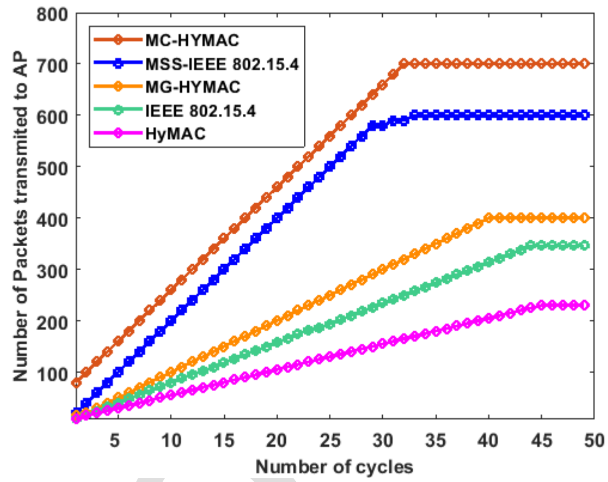

Fig. 18. Number of packets received (throughput) based on the number of cycles.

delays during CCA, back-off periods, waiting for acknowledgment, and so on. In addition, devices can experience delays during CAP when the channel idle probability is low. Therefore, for each failed channel attempt, the unit back duration is doubled, which would require extra energy for the channel to be reaccessed again. In practice, this process requires additional energy and results in a delay in packet transmission. We addressed this problem in the proposed MC-HYMAC protocol by designing a back-off time scheme and channel-selection mechanism for efficient channel utilization. In addition, in the proposed MC-HYMAC protocol, the $\mathcal{D}$ devices are allocated a specific time slot in the EAP as they need to transmit their emergence-based packets as urgently as possible without having to contend for channel access opportunities to enable the successful delivery of their health packets and minimize delay. The proposed MC-HYMAC protocol outperforms the existing MSS-IEEE 802.15.4, MG-HYMAC, IEEE 802.15.4, and HyMAC protocols in terms of delay reduction. As an example, for the first back-off period, as shown in Fig. 14, when the number of devices is 7, the MC-HYMAC protocol outperforms existing protocols with a delay reduction of approximately 1%.

E. Investigation of the Total Number of Health Packets Dropped and the Total Number of Received Health Packets

In this section, we investigate the performance of the MC-HYMAC protocol based on the total number of health packets dropped and the total number of health packets successfully received at the AP, that is, throughput, and compare it with existing protocols, such as MSS-IEEE 802.15.4, MG-HYMAC, IEEE 802.15.4, and HyMAC. Consequently, we performed different simulation experiments with different numbers of cycles, as shown in Figs. 17 and 18.

In practice, it is possible that the total number of health packets transmitted by the devices is not the same as the total number of health packets received by the AP owing to the packet drop issue. Based on this fact, we analyzed the total number of dropped health packets during transmission for the proposed MC-HYMAC and the existing protocols by employing a uniform random model, where the probability of a good link is 70% and the probability of a bad link is 30%. From Fig. 16, we observe that the number of packets dropped when the proposed MC-HYMAC was enabled was lower than that of the existing protocols. As an example, in cycle 35, the MC-HYMAC protocol achieved an improvement of approximately 10% over the MSS-IEEE 802.15.4, 19% over the MG-HYMAC protocol, 45% over the IEEE 802.15.4, and 49% over the HyMAC protocols.

Throughput is determined by computing the total number of health packets that are successfully received at the AP. From Fig. 18, we can infer that the proposed MC-HYMAC protocol has a higher number of packets successfully received at the AP than the existing protocols. For example, in cycle 35, MC-HYMAC achieved a significant improvement of approximately 14% over MSS-IEEE 802.15.4, 50% over MG-HYMAC, 63% over IEEE 802.15.4, and 75% over HyMAC.

F. Investigation of the Impact of Transmission Probability on the Lifetime of the Devices

The impact of transmission probability on the device's lifetime is presented in this section. To achieve this, different experiments were performed on the proposed MC-HYMAC protocol and MSS-IEEE 805.15.4, MG-HYMAC, IEEE 802.15.3, and HyMAC protocols. We set the five protocols to ten devices and battery power to 1200 J. In addition, we set the $\mathcal{D}$ devices to 4, while the $\mathcal{G}$ devices are set to 6, and the outcomes of the simulation experiments are presented in Fig. 19. From Fig. 19, we can infer that, as the transmission probability increases, the device lifetime decreases for all protocols. However, the proposed MC-HYMAC protocol performed better than the existing protocols. For instance, when the transmission probability was set to 0.8, the proposed MC-HYMAC protocol achieved a significant improvement of approximately 10% over the MSS-IEEE 802.15.4 protocol, 21% over the MG-HYMAC protocol, 39% over the IEEE 802.15.4 protocol, and 45% over the HyMAC protocol. The improvement achieved by the MC-HYMAC protocol is due to the multichannel concept, the channel selection mechanism, the back-off time scheme, the time-slot management scheme,

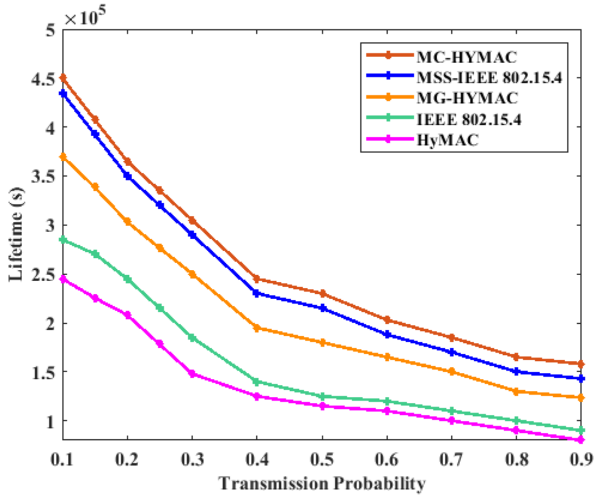

Fig. 19. Impact of devices lifetime versus transmission probability.

and the adaptive power allocation scheme that we employed, which minimizes energy consumption and delays, improves channel utilization efficiency and throughput, and prolongs the lifetime of the devices.

VIII. Conclusion

This article addresses the energy consumption, time-slot management, delay, and channel utilization issues in a WBAN system. To address these issues, we propose a multichannel concept in which the AP and the devices use separate channels for communication. To efficiently utilize the channels, a channel-mapping mechanism and a channel-selection policy were introduced. The mechanism helped the devices know when to transmit their health packets, thus improving the energy efficiency, throughput, and overall lifetime of the network. In addition, a back-off time policy scheme, a time-slot management scheme, and an adaptive power control scheme were designed to minimize energy wastage and time-slot wastage, and enhance channel utilization efficiency. Furthermore, we propose a finite-state discrete-time Markov model to identify the traffic arrival pattern of the devices, analyze the state transitions of the devices, and analyze the state of the channel for decision-making purposes to improve the lifetime of the network. The proposed MC-HYMAC protocol was validated and compared with some existing MAC protocols, including the MSS-IEEE 802.15.4, MG-HYMAC, IEEE 802.15.4, and HyMAC protocols, based on their energy efficiency, delay, packet drop and received ratio, and device lifetime. Consequently, MC-HYMAC performed better than MSS-IEEE 802.15.4, MG-HYMAC, IEEE 802.15.4, and HyMAC.

References

[1] D. D. Olatinwo, A. Abu-Mahfouz, and G. Hancke, “A survey on LPWAN technologies in WBAN for remote health-care monitoring,” *Sensors*, vol. 19, no. 23, p. 5268, Nov. 2019.

[2] C. A. Tokognon, B. Gao, G. Y. Tian, and Y. Yan, “Structural health monitoring framework based on Internet of Things: A survey,” *IEEE Internet Things J.*, vol. 4, no. 3, pp. 619–635, Jun. 2017.

[3] S. O. Olatinwo and T. H. Joubert, “Energy-efficiency maximization in a wireless powered IoT sensor network for water quality monitoring,” *Comput. Netw.*, vol. 176, no. 1, pp. 1–10, Jul. 2020.

[4] L. D. Xu, W. He, and S. Li, “Internet of Things in industries: A survey,” *IEEE Trans. Ind. Informat.*, vol. 10, no. 4, pp. 2233–2243, Nov. 2014.

[5] D. D. Olatinwo, A. M. Abu-Mahfouz, and G. P. Hancke, “Towards achieving efficient MAC protocols for WBAN-enabled IoT technology: A review,” *EURASIP J. Wireless Commun. Netw.*, vol. 2021, no. 1, pp. 1–47, Mar. 2021.

[6] D. D. Olatinwo, A. M. Abu-Mahfouz, and G. P. Hancke, “A hybrid multi-class MAC protocol for IoT-enabled WBAN systems,” *IEEE Sensors J.*, vol. 21, no. 5, pp. 6761–6774, Mar. 2021.

[7] Y. Chu, P. D. Mitchell, and D. Grace, “ALOHA and Q-learning based medium access control for wireless sensor networks,” in *Proc. Int. Symp. Wireless Commun. Syst. (ISWCS)*, Aug. 2012, pp. 511–515.

[8] R. Pace et al., “Inter-health: An interoperable IoT solution for active and assisted living healthcare services,” in *Proc. IEEE 5th World Forum Internet Things*, Apr. 2019, pp. 81–86.

[9] M. Salayma, A. Al-Dubai, I. Romdhani, and Y. Nasser, “Reliability and energy efficiency enhancement for emergency-aware wireless body area networks (WBANs),” *IEEE Trans. Green Commun. Netw.*, vol. 2, no. 3, pp. 804–816, Sep. 2018.

[10] D. D. Olatinwo, A. M. Abu-Mahfouz, G. P. Hancke, and H. C. Myburgh, “Energy efficient priority-based hybrid MAC protocol for IoT enabled WBAN systems,” *IEEE Sensors J.*, vol. 23, no. 12, pp. 13524–13538, May 2023.

[11] D. D. Olatinwo, A. M. Abu-Mahfouz, and G. P. Hancke, “Energy-aware hybrid MAC protocol for IoT enabled WBAN systems,” *IEEE Sensors J.*, vol. 22, no. 3, pp. 2685–2699, Feb. 2022.

[12] L. Aissaoui Ferhi, K. Sethom, and F. Choubani, “Energy efficiency optimization for wireless body area networks under 802.15.6 standard,” *Wireless Pers. Commun.*, vol. 109, no. 3, pp. 1769–1779, Dec. 2019.

[13] T. Samal and M. R. Kabat, “A prioritized traffic scheduling with load balancing in wireless body area networks,” *J. King Saud Univ.-Comput. Inf. Sci.*, vol. 34, no. 8, pp. 5448–5455, Sep. 2022.

[14] M. Ambigavathi and D. Sridharan, “Traffic priority based channel assignment technique for critical data transmission in wireless body area network,” *J. Med. Syst.*, vol. 42, no. 11, pp. 1–19, Nov. 2018.

[15] R. Zhang, H. Moungla, J. Yu, and A. Mehaoua, “Medium access for concurrent traffic in wireless body area networks: Protocol design and analysis,” *IEEE Trans. Veh. Technol.*, vol. 66, no. 3, pp. 2586–2599, Mar. 2017.

[16] X. Yang, L. Wang, and Z. Zhang, “Wireless body area networks MAC protocol for energy efficiency and extending lifetime,” *IEEE Sensors Lett.*, vol. 2, no. 1, pp. 1–4, Mar. 2018.

[17] G. Sun, K. Wang, H. Yu, X. Du, and M. Guizani, “Priority-based medium access control for wireless body area networks with high-performance design,” *IEEE Internet Things J.*, vol. 6, no. 3, pp. 5363–5375, Jun. 2019.

[18] P. Thirumoorthy, P. Kalyanasundaram, R. Maheswar, P. Jayarajan, G. R. Kanagachidambaresan, and I. S. Amiri, “Time-critical energy minimization protocol using PQM (TCEM-PQM) for wireless body sensor network,” *J. Supercomput.*, vol. 76, no. 8, pp. 5862–5872, Aug. 2020.

[19] K. Cho, Z. Jin, and J. Cho, “Design and implementation of a single radio multi-channel MAC protocol on IEEE 802.15.4 for WBAN,” in *Proc. 8th Int. Conf. Ubiquitous Inf. Manage. Commun.*, Jan. 2014, pp. 1–8.

[20] C. Li, B. Zhang, X. Yuan, S. Ullah, and A. V. Vasilakos, “MC-MAC: A multi-channel based MAC scheme for interference mitigation in WBANs,” *Wireless Netw.*, vol. 24, no. 3, pp. 719–733, Apr. 2018.

[21] I. Kirbas, A. Karahan, A. Sevin, and C. Bayilmis, “isMAC: An adaptive and energy-efficient MAC protocol based on multi-channel communication for wireless body area networks,” *KSII Trans. Internet Inf. Syst.*, vol. 7, no. 8, pp. 1805–1824, 2013.

[22] N. Li, X. Cai, X. Yuan, Y. Zhang, B. Zhang, and C. Li, “EIMAC: A multi-channel MAC protocol towards energy efficiency and low interference for WBANs,” *IET Commun.*, vol. 12, no. 16, pp. 1954–1962, Oct. 2018.

[23] T. Samal and M. R. Kabat, “Energy-efficient time-sharing multichannel MAC protocol for wireless body area networks,” *Arabian J. Sci. Eng.*, vol. 47, no. 2, pp. 1791–1804, Feb. 2022.

[24] M. B. Rasheed, N. Javaid, M. Imran, Z. A. Khan, U. Qasim, and A. Vasilakos, “Delay and energy consumption analysis of priority guaranteed MAC protocol for wireless body area networks,” *Wireless Netw.*, vol. 23, no. 4, pp. 1249–1266, May 2017.

[25] D. D. Olatinwo, A. Abu-Mahfouz, G. Hancke, and H. Myburgh, “IoT-enabled WBAN and machine learning for speech emotion recognition in patients,” *Sensors*, vol. 23, no. 6, p. 2948, Mar. 2023.

[26] B. Zhang, C. Li, Z. Liu, X. Yuan, and L. Yang, "On energy-delay efficiency for WBAN: A multi-channel scheme," in *Proc. IEEE/CIC Int. Conf. Commun. China (ICCC)*, Nov. 2015, pp. 1–5.

[27] K. G. Mkongwa, C. Zhang, and Q. Liu, "A reliable data transmission mechanism in coexisting IEEE 802.15.4-beacon enabled wireless body area networks," *Wireless Pers. Commun.*, vol. 128, pp. 1–22, Sep. 2022.

[28] H. Alshaheen and H. Takruri-Rizk, "Energy saving and reliability for wireless body sensor networks (WBSN)," *IEEE Access*, vol. 6, pp. 16678–16695, 2018.

[29] J. F. Hayes and T. V. G. Babu, *Modeling and Analysis of Telecommunications Networks*. Hoboken, NJ, USA: Wiley, 2004.

[30] Z. Liu and I. Elhanany, "RL-MAC: A reinforcement learning based MAC protocol for wireless sensor networks," *Int. J. Sensor Netw.*, vol. 3, no. 4, pp. 117–124, Jan. 2006.

[31] A. Saboor, R. Ahmad, W. Ahmed, A. K. Kiani, Y. L. Moullec, and M. M. Alam, "On research challenges in hybrid medium-access control protocols for IEEE 802.15.6 WBANs," *IEEE Sensors J.*, vol. 19, no. 19, pp. 8543–8555, Oct. 2019.

[32] R. Khan, M. M. Alam, and M. Guizani, "A flexible enhanced throughput and reduced overhead (FETRO) MAC protocol for ETSI SmartBAN," *IEEE Trans. Mobile Comput.*, vol. 21, no. 8, pp. 2671–2686, Aug. 2022.

[33] K. G. Mkongwa, Q. Liu, and S. Wang, "An adaptive backoff and dynamic clear channel assessment mechanisms in IEEE 802.15. 4 MAC for wireless body area networks," *Ad Hoc Netw.*, vol. 120, pp. 1–15, Sep. 2021.

[34] S. Henna and M. A. Sarwar, "An adaptive backoff mechanism for IEEE 802.15.4 beacon-enabled wireless body area networks," *Wireless Commun. Mobile Comput.*, vol. 2018, pp. 1–15, Jun. 2018.

[35] P. Le-Huy and S. Roy, "Low-power 2.4 GHz wake-up radio for wireless sensor networks," in *Proc. IEEE Int. Conf. Wireless Mobile Comput., Netw. Commun.*, Oct. 2008, pp. 13–18.

[36] M. H. S. Gilani, I. Sarrafi, and M. Abbaspour, "An adaptive CSMA/TDMA hybrid MAC for energy and throughput improvement of wireless sensor networks," *Ad Hoc Netw.*, vol. 11, no. 4, pp. 1297–1304, Jun. 2013.

[37] W. Wang, H. Wang, D. Peng, and H. Sharif, "An energy efficient pre-schedule scheme for hybrid CSMA/TDMA MAC in wireless sensor networks," in *Proc. 10th IEEE Singap. Int. Conf. Commun. Syst.*, Mar. 2006, pp. 1–5.

[38] I. Rhee, A. Warrier, M. Aia, and J. Min, "Z-MAC: A hybrid MAC for wireless sensor networks," in *Proc. 3rd Int. Conf. Embedded Networked Sensor Syst.*, 2005, pp. 90–101.

[39] V. Nguyen, T. Z. Oo, P. Chuan, and C. S. Hong, "An efficient time slot acquisition on the hybrid TDMA/CSMA multichannel MAC in VANETs," *IEEE Commun. Lett.*, vol. 20, no. 5, pp. 970–973, May 2016.

[40] S. O. Olatinwo and T. H. Joubert, "Efficient energy resource utilization in a wireless sensor system for monitoring water quality," *EURASIP J. Wireless Commun. Netw.*, vol. 2019, no. 1, pp. 1–22, Dec. 2019.

[41] S. Olatinwo and T.-H. Joubert, "Optimizing the energy and throughput of a water-quality monitoring system," *Sensors*, vol. 18, no. 4, p. 1198, Apr. 2018.

[42] R. Piyare, A. L. Murphy, C. Kiraly, P. Tosato, and D. Brunelli, "Ultra low power wake-up radios: A hardware and networking survey," *IEEE Commun. Surveys Tuts.*, vol. 19, no. 4, pp. 2117–2157, 4th Quart., 2017.

[43] A. D. Shoaei, M. Derakhshani, S. Parsaeefard, and T. Le-Ngoc, "Learning-based hybrid TDMA-CSMA MAC protocol for virtualized 802.11 WLANs," in *Proc. IEEE 26th Annu. Int. Symp. Pers., Indoor, Mobile Radio Commun. (PIMRC)*, Aug. 2015, pp. 1861–1866.

Damilola D. Olatinwo is a researcher and an academician, who has research expertise in the mathematical modeling of problems in research areas, such as the Internet of Things, wireless body area networks, healthcare monitoring, machine-to-machine communications, and low-power and long-range communication systems. Her research expertise also includes the design of resource management strategies, communication protocols, the application of artificial intelligence techniques, and the development of stochastic probability models.

Adnan M. Abu-Mahfouz (Senior Member, IEEE) received the M.Eng. and Ph.D. degrees in computer engineering from the University of Pretoria, Pretoria, South Africa, in 2005 and 2011, respectively.

He is currently a Chief Researcher and the Centre Manager of the Emerging Digital Technologies for 4IR (EDT4IR) Research Centre, Council for Scientific and Industrial Research, Pretoria; an Extraordinary Professor with the University of Pretoria; a Professor Extraordinaire with the Tshwane University of Technology, Pretoria; and a Visiting Professor with the University of Johannesburg, Johannesburg, South Africa. His research interests are wireless sensor and actuator networks, low-power wide area networks, software-defined wireless sensor networks, cognitive radio, network security, network management, and sensor/actuator node development.

Prof. Abu-Mahfouz is the Section Editor-in-Chief of the *Journal of Sensor and Actuator Networks*, an Associate Editor at IEEE INTERNET OF THINGS JOURNAL, IEEE TRANSACTIONS ON INDUSTRIAL INFORMATICS, IEEE TRANSACTIONS ON CYBERNETICS, IEEE ACCESS, and *Frontiers in Plant Science*, and a member of many IEEE technical communities.

Gerhard P. Hancke (Fellow, IEEE) received the B.Eng. and M.Eng. degrees in computer engineering from the University of Pretoria, Pretoria, South Africa, in 2002 and 2003, respectively, and the Ph.D. degree in computer science from the Security Group, Computer Laboratory, University of Cambridge, Cambridge, U.K., in 2008.

He worked at the Smart Card and IoT Security Centre and the Department of Information Security, Royal Holloway, University of London, Egham, U.K. He is currently a Professor with the Department of Computer Science, City University of Hong Kong, Hong Kong. His research interests are the security and resilience of communication, localization, and distributed sensing within the Industrial Internet of Things.

Hermanus C. Myburgh (Member, IEEE) received the B.Eng., M.Eng., and Ph.D. degrees in computer and electronic engineering from the University of Pretoria, Pretoria, South Africa, in 2007, 2009, and 2013, respectively.

He is an Associate Professor with the Department of Electrical, Electronic, and Computer Engineering, University of Pretoria. He is the Head of the Advanced Sensor Networks (ASN) Research Group. He is a Co-Founder and a Scientific Advisor to a South African digital health company, hearX Group (Pty) Ltd. He is the inventor of a number of smartphone-based hearing assessment solutions. His research interests are in wireless communication, sensor fusion, machine learning, and mobile health.